1966

# The Effect of Wave Shape on the Electrical Breakdown of Nitrogen Gas

Keith E. Crouch

# THE EFFECT OF WAVE SHAPE ON THE ELECTRICAL BREAKDOWN OF NITROGEN GAS

BY

KEITH E. CROUCH

A thesis submitted
In partial fulfillment of the requirements for the
degree Master of Science, Department of
Electrical Engineering, South
Dakota State University

June, 1966

THE EFFECT OF WAVE SHAPE ON THE ELECTRICAL BREAKDOWN OF NITROGEN GAS

This thesis is approved as a creditable and independent investigation by a candidate for the degree, Master of Science, and is acceptable as meeting the thesis requirements for this degree, but without implying that the conclusions reached by the candidate are necessarily the conclusions of the major department.

Thesis Adviser Date

Head, Electrical Engineering Department Date

## ACKNOWLEDGMENTS

The author wishes to express his appreciation and gratitude to Prof. L. C. Whitman, whose guidance and advice made this investigation possible. Also thanks go to the Dean, M. L. Manning, for obtaining the support for this project.

The author also wishes to express his thanks to Prof. George H. Duffey for the advice given on numerable occasions.

K.E.C.

TABLE OF CONTENTS

## LIST OF TABLES

## LIST OF FIGURES

# INTRODUCTION

## A. Brief History of Lightning Knowledge and Work

Man's basic interest in high voltage gaseous discharges probably began in the caves of early caveman thousands of years ago as he looked out into the storms and observed the lightning. Through the years, he built up a fear of this unknown and powerful force of nature. It was Ben Franklin who first showed that the lightning of the skies was the same electricity produced by a Leyden jar or static generator.

However, lightning remained just a terrible phenomenon that one protected oneself against using Franklin's lightning rods, with little else known or cared about it until the end of the 19th century. Man then began to study lightning in earnest because he had started transmitting electrical power over transmission lines which were subject to lightning strokes. These lines had to be protected from the lightning and, to protect them, more had to be known about the behavior and characteristics of lightning strokes. Methods also had to be devised to test the safeguards that were installed to prove they would really work.

The first engineering study of lightning was undertaken by Steinmetz and his coworkers at Schenectady, New York. He built the first artificial lightning generator in

1923 at his laboratory and used it to investigate and observe the effects of controlled lightning strokes.

Steinmetz's work was followed by that of F. W. Peek, Jr. at Pittsfield, Massachusetts. Using the description of a new type of lightning generator developed by E. Marx in 1925, Peek started building bigger and bigger generators with which to test apparatus.

At this same time, many investigators took to the field to observe and take measurements on natural lightning, wherever they were able to find it. As a result of these investigations, standards of insulation levels and specifications of protective devices were established.[1]

The investigations suggested that testing of equipment could be carried out using laboratory lightning generators. The voltage wave that was standardized was one which reached its crest peak in one and one-half microseconds and fell back to one-half of crest in 40 microseconds, both times measured from the virtual zero of the wave. The methods of obtaining these voltage waves and how measurements are to be made are given in the AIEE Standards.[2]

These methods of determining whether or not a piece of power apparatus is safe for general use on transmission lines have been used with much success for the last 30 years or more. However, with the advent of much higher transmission voltages and much larger systems being used for

economical reasons, new problems arose.

B. The Switching Surge Problem

When sections of these large systems are switched into or out of the systems, inductive voltages are created in accordance with Lenz's law. These changes in operating conditions bring about voltage surges that travel on the lines. These surges are known as switching surges. The voltages present in a switching surge may be several times the operating voltage level of the line on which it occurs. In this respect, the surge is much like a lightning voltage, but in other respects, the surges are very different from lightning waves. While a lightning pulse reaches crest in one and one-half microseconds, the switching surge may take as long as 1000 microseconds. A typical lightning wave is back down to one-half crest in 40 microseconds, but a switching surge may stay within 90% of crest value for as long as 200 microseconds. These facts about switching surges have been known for some time and it has been generally assumed that a ratio of 1.3 between switching surge strength of apparatus and low frequency crest voltage strength was satisfactory for adequate protection.

The voltage waves that have been discussed so far are imposed on the whole electric power distribution systems and, to some degree, on the insulation of each component.

Since most transformers and switchgear are in oil-filled cases, extensive work in the testing of these oils has been done.

C. Application to Gases

Lately an interest has been generated in using electro-negative gases as an insulating medium because of their greater electric strength as compared to air. Testing has been carried on with such gases as $C_3F_8$, $C_4F_8$, $SF_6$ and $NF_3$. These tests have been carried out using 60 cycle and lightning impulse voltages.[3,4,5]

The next logical step is to extend the work by covering the gap between these two extremes of 60 cycle and lightning waves. This range would cover switching surges and compare their breakdown strengths to the two extremes. This type of work has been done for oil and solid insulations, but very little has been done in the intermediate range with gases.[6]

Since, in gases, there are a variety of things that can influence the character of breakdown, as will be discussed shortly, the most meaningful way to proceed is by experimental comparison between gases.

Identical conditions are set up and tests are conducted on both electro-negative gases and a standard gas, usually air. The results of these tests give direct compari-

sons of relative strengths of resistance to electrical breakdown of the particular gases.

## D. The Aim of This Thesis

The problem considered in this paper is the establishment of a criterion, namely the electric strength of nitrogen (or its approximate equivalent air), over a wide spectrum of wave shapes by which tests on the electro-negative gases can be evaluated.

Thus, the specific problem dealt with in this paper is how the breakdown character of nitrogen gas changes as the shape of the impulse wave is varied. The variation in waveform used here was obtained by changing the rise time and time back to one-half crest of the wave. These times were varied over a region of rise times of 0.5 to 550 microseconds and time back to one-half crest of 10 up to 9000 microseconds.

# LITERATURE REVIEW

## A. Evaluation of New Insulation by Comparison

Engineers who are responsible for building electrical power systems have found the required levels of insulation in their systems mostly by experimentation. New types of insulation or insulating systems must be tested and the results compared to results of tests on materials currently in use. Standard test procedures have been established to make it easier for meaningful comparisons to be made. These procedures bypass the necessity of finding absolute insulation strengths of the new material or system under all conditions that might be encountered. The abilities of the older materials are generally known and the new material is rated in terms of the old. There are many examples of this type of work cited in the literature. The engineer uses this knowledge of relative strengths in determining what materials he should use in his design of equipment.

Much interest has also been shown in the theoretical aspects of breakdown. The interest of this paper is in gaseous breakdown and the work in this area alone consists of many volumes. An extensive bibliography of those works would be longer than this paper. The references used in this paper are not meant to be more than merely representa-

tive of these works. For a more comprehensive study, the reader is referred to the bibliographies of the references cited herein.

## B. Theories of Gaseous Breakdown

There have been two main theories of gaseous breakdown set forth in the literature. Following is a brief explanation of each along with a discussion of the shortcomings of each. No absolute predictions of the value of the breakdown voltage can be made concerning the topic of this paper. However, these theories will be helpful in analyzing the results of the present experiment.

### 1. The Townsend Theory

The first major investigation of the conduction of electricity through gases was carried out by J. S. Townsend around 1900. The results of this work were set forth by him in various articles and a book.[7] Townsend's concept was that the field applied to the gas caused free ions in the gas to move toward the respective positive and negative electrodes which established the field. These free ions are present in the gas due to cosmic radiation, photo-ionization and other sources. When the ions are accelerated by a large enough field, their collisions with other gas atoms will cause new ions. He assumed the gas was ionized by both positive and negative ions. It was shown later that

the negative ions are actually free electrons.[8] His equation is:

$$I = I_o \frac{(\alpha-\beta)e^{(\alpha-\beta)d}}{\alpha-\beta e^{(\alpha-\beta)d}} \qquad (1)$$

where I is current between the electrodes, $I_o$ is the photoelectric or ionic current in the gap, d is the gap length, $\alpha$ is the number of new ions created in the gas per centimeter of travel along field axis by an initial electron, and $\beta$ is the number of new ions created by the advance of a positive ion one centimeter along the field axis. This equation is able to give satisfactory results for small gaps and low pressures. It was shown later that the electrons are the active participants in the breakdown. Consequently $\alpha$ and $\beta$ were redefined to specifically relate to the number of electrons created per centimeter of travel.

Two other equations were later written by Loeb as modifications of Townsend's original equation because it was found that electrode materials affected breakdown points. The equations are:

$$I = I_o \frac{e^{\alpha d}}{1-\gamma(e^{\alpha d}-1)} \qquad (2)$$

$$I = I_o \frac{\alpha e^{\alpha d}}{\alpha-\eta\theta g(e^{(\alpha-\mu)d}-1)} \qquad (3)$$

In equation (2), $\gamma$ is the chance that electrons will be liberated from the cathode by positive ion bombardment.

All other terms are as previously defined. In equation (3) $\theta$ is the number of photons, created per centimeter of advance by an initial electron, whose frequency will be such that they could liberate an electron from the cathode; g is a geometrical factor of about 0.5 which gives the fraction of photons in the gap which reach the cathode; $\eta$ is the fraction of photons reaching the cathode which actually liberate electrons into the gas; and $\mu$ is the adsorption coefficient of the photons in the gas. With properly determined coefficients, these equations give much the same results as Townsend's equation. Also it was shown that $\beta$ is negligible in gases at field strengths needed for actual breakdowns. The criterion that Townsend gave for sparking was that the denominator of equation (1) go to zero:

$$\frac{\alpha}{\beta} = e^{(\alpha-\beta)d} \tag{4}$$

or assuming $\beta$ small,

$$e^{\alpha d} = \frac{\alpha}{\beta} \tag{4a}$$

This singularity was interpreted to mean that the current increased without limit and breakdown occurred. In equations (2) and (3), the denominator was also set equal to zero as a criterion for sparking.[9]

Most of Townsend's work was done with laboratory

apparatus that was considered very crude by standards of 10-15 years later. Consequently, as equipment improved, errors in Townsend's work were found and his theory was not able to stand as first stated. However, Townsend refused to modify the theory or to accept data showing his theory inadequate.

The major stumbling block to Townsend's theory are discharges at gas pressures near atmospheric pressure. The process described by him would take several crossings of electron avalanches before the gap is sufficiently ionized to be a free conductor. It was found in subsequent experiments that the time of formation of the spark is insufficient to allow more than one crossing. This high speed of formation of the spark is such that the positive ions in the gap do not have time to move.[10,11]

Many other less significant problems were encountered with Townsend's theory and are discussed in the literature cited in this paper, especially in the works of Loeb. It suffices here to say these problems made Townsend's theory unacceptable for many people. Many of these problems were overcome, in part, by a different theory presented in 1941 by Loeb and Meek. This theory was called the Streamer Theory of Electrical Breakdown.

2. The Streamer Theory

In the Streamer Theory, the process is started by

an electron avalanche, the same as Townsend's spark. This avalanche leaves behind the positive ions which form in a conical shape. The cone is smallest at cathode side and grows larger as the avalanche approaches the anode. These positive ions are the source of a space charge in the gap. This space charge tends to intensify the field gradient between the charge and the cathode. The electrons in the initial avalanche will collide with gas atoms and excite them. Some of the excited atoms will give off electrons and others will give off photons of various energies (frequencies). Due to these excited atoms, the whole region between the electrodes will be subjected to a shower of photons. Some of these photons will contain enough energy to photo-ionize atoms and cause them to give off electrons. In the gap region, there is a source of new photo-electrons. A part of this source will be between the space charge and the cathode. The electrons nearest the space charge will be drawn into it. The positive ions the photo-electrons leave behind will move the channel of the space charge closer to the cathode. The electrons that are pulled into the channel will reduce the effect of the space charge on the parent or first avalanche so it will continue until it reaches the anode. At the same time, however, the space-charge channel will be propagating itself across the gap from the anode to the cathode. This space charge channel is a plasma of

conducting charges and is called the streamer.

The criterion that Loeb and Meek set for determining if the streamer would propagate or die out was whether or not the field at the surface of the streamer was equal to the impressed field. If the field was less than the impressed field, the photo-electrons would not be drawn into the streamer channel. Meek set the space charge field,

$$X_1 = KX_s \tag{5}$$

where $X_s$ is the impressed field, $X_1$ is space charge field and K is a constant which varies from $0.1 < K < 1.0$. If K is too small, the streamer will not propagate. Loeb and Meek set $K = 1.0$. Then they worked backward and came up with the following equation for breakdown:

$$\alpha d + \log_e \frac{\alpha_A}{p} = 14.46 + \log_e \frac{X_s}{p} + \frac{1}{2} \log_e \frac{d}{p} \tag{6}$$

Here $\alpha$ is the first Townsend coefficient; d is the gap length; p is the gas pressure; $X_s$ is potential gradient of the gap needed for breakdown, which is the unknown; and the constant 14.46 is dependent on K and the ionization radius of the space charge front. Its determination is not given here but can be studied in the book by Loeb and Meek which is cited. The equation can be solved by trial and error to yield a value of $\frac{X_s}{p}$. Then

$$V_s = \frac{X_s}{p} pd. \tag{7}$$

The equation given here is for a uniform field and atmospheric pressure. The equation can be varied for other fields and pressures. A change in the field and the pressure will change factors influencing the space charge radius, therefore, changing the constant factor 14.46.[12]

3. The Raether Theory

The theory presented by Loeb and Meek was paralleled very closely by H. Raether, who was working independently of Loeb and Meek. There were some differences in the presentation of the two theories. Raether's criterion for breakdown was that

$$e^{\alpha d} = N_1 = \text{constant}. \qquad (8)$$

He chose $N_1$ as an emperical value for the constant and proceeded to find d, the distance needed. This was, of course, strictly an emperical method but was merged with the Streamer Theory as will be shown.[13]

4. Modifications of the Streamer Theory

The Streamer Theory was criticized on several counts. The constant in the equation depends on a value of K which is arbitrarily chosen. Also the equation does not depend in any way on what materials are used for electrodes.

It was also pointed out that the manner in which the space charge acts was assumed and it might not really act in that manner. Therefore, the photo-electrons might not be drawn into the channel as supposed. It was also assumed

that α remained constant at any point throughout the gap when the ion densities and consequently the field of the channel was calculated. This was not so because α depends on the field applied.

Also, it was pointed out that Raether's criterion, $e^{\alpha d}$ = constant = $10^9$, gave essentially the same results as Meek's equation. This suggested that a modified Townsend equation could be set up, such as:

$$I = I_o \frac{e^{\alpha d}}{1-\left(\frac{\omega}{\alpha}\right)(e^{\alpha d}-1)} \tag{9}$$

$$\omega = \delta + \gamma + \beta \tag{10}$$

Here δ is electron emission from the cathode caused by impact of photons and the other terms are as defined previously. The condition that $1-\left(\frac{\omega}{\alpha}\right)(e^{\alpha d}-1) = 0$ is the condition that essentially $e^{\alpha d}$ = constant. This is Raether's criterion and could hold just as well as Meek's.[14] In fact, with some manipulations, Meek's equation can easily be put in this same form.

$$\text{In} \qquad \alpha d + \log_e \frac{\alpha_A}{p} = 14.46 + \log_e \frac{X_s}{p} + \log_e \left(\frac{d}{p}\right)^{1/2}$$

$$\text{let } \log_e C_1 = 14.46$$

$$e^{\alpha d} = \frac{C_1\left(\frac{X_s}{p}\right)\left(\frac{d}{p}\right)^{1/2}}{\left(\frac{\alpha_A}{p}\right)} = \frac{C_1 X_s}{\alpha_A}\left(\frac{d}{p}\right)^{1/2} = \text{constant} \tag{11}$$

Here $X_s$ is arbitrarily chosen, as it is in Meek's equation and $\alpha_A$ is Townsend's first coefficient at the anode.

That the preceding criticisms were true was readily accepted by Meek and Loeb. The real significance of the Streamer Theory did not lie in its mathematical exactness but in that it endeavored to present a better physical picture of what was happening.

5. The Presently Held Theory

As can be seen by the preceding discussion, the actual mechanism of the breakdown is probably a combination of the Townsend and Streamer type of formations. This view is the one that is presently held by most experts in the field. The breakdown starts with an avalanche and if the overvoltage is small, a Townsend type mechanism occurs. If the voltage is higher, the space charge left by the avalanche will be strong enough to initiate the streamer mechanism. The theories were formulated for uniform fields and static voltages. For conditions of high overvoltage and non-uniform fields, the theories are extended or extrapolated to cover these regions. This means that the predictions of the breakdown voltage become very inaccurate. The equations cited are very heavily dependent on values of $\alpha$, $\beta$, $\gamma$, $\delta$, $\mu$, etc.[15, 16]

These ionization coefficients are functions of the fields, pressure and several other factors of less import-

ance. Their values are not yet completely determined in most areas. The streamer idea is well enough accepted that several investigators have and are trying to evaluate these coefficients more precisely.[17] For more extensive information on these coefficients, the reader is referred to references 9, 11, 16, 31, 32 and 33 in which work on these problems is discussed.

6. Peek's Contribution

The concern of this paper is with impulse breakdown in non-uniform fields. The aforementioned theories can be used here but several inadequacies are present when overvoltages and fast rising pulses are used.

The usual manner in which fast rising wave fronts are to be treated was first suggested by Peek. The key to the question is that in the theories of breakdown, the process is started by initial electrons present in the gap. When the voltage reaches the static breakdown point and no electrons are present, some time will elapse before the electrons can be produced. During this time, the voltage will reach some peak above the static point. The ratio of this peak to the static voltage needed is termed the impulse ratio. Based on this idea, some conclusions about the height of wave at breakdown could be made knowing the steepness of the wave front and the time for the electrons to appear.[18]

In later studies, it was shown that the time that elapsed after the voltage passed static breakdown until the actual breakdown process started was a statistical function of external ionization factors. This time lag of the system was called the statistical time lag. The time taken by the breakdown formation was called the formative time lag. The statistical time lag was shown to be a function of external irradiation, which is a time dependent phenomenon.[19]

7. Hagenguth's Volt-Time-Area Criterion

In 1941, Hagenguth reported that the rise time of the wave used had an effect on the statistical time lag of the gap under test. Up to this time, it was assumed that the lag was not related to the voltage wave. This had been the basis for constructing volt-time plots. These plots showed the crest voltage versus time to spark over irrespective of what the risetime of the applied voltage wave was. Hagenguth proposed that volt-time-area plots be made instead of just volt-time curves. These volt-time-area curves were obtained by plotting the ratio of $t_1$ time to crest of the wave, to $t_2$ time to breakdown of wave, both measured from time zero of the wave, versus spark-over voltage of the wave. Hagenguth assumed that the time to spark over of the wave was a function of the rise time only and the statistical nature of the time lag was neglected. He limited

his results to waves that rose to crest in less than 6-10 microseconds. He recognized his proposal to be empirical and correct only over a small range of waves.[20]

The statistical time lag was also found to depend on the electrode surface condition and electrode material. A set of electrodes which are greasy or coated with oxides will have longer time lags than those which are cleaned and polished. Electrodes made of aluminum or magnesium have shorter time lags than electrodes of copper or copper oxide.

By using clean electrodes of proper materials, irradiating them and the gap with intense radiation (mercury lamp or radioactive materials, etc.), and using steep front waves, the statistical time lags of a gap can be made very short. Time lags on the order of $10^{-9}$ seconds, statistical plus formative, have been observed using these methods. At the other extreme, lags of seconds have also been recorded.[21]

It can be seen that the statistical time lag is really a function of many variables. Due to the large number of these variables, which is probably greater than yet recognized, no determination of the relationship has been formulated.

8. A Breakdown Theory for Non-Uniform Fields

An attempt has been made to formulate a criterion for calculating breakdown under non-uniform fields and impulse voltage waves. Earlier Meek's equation was shown to be in a form much like Raether's, which was

$$e^{\alpha d} = \frac{C_1 E_s}{\alpha_A} = \text{constant}$$

If the field is not uniform across the gap, $\alpha$ will vary since it depends on the field. This variation can be found and has been plotted. The equation can be varied to allow for this to get

$$e^{\int_0^d \alpha(x)dx} = \frac{C_1 E_s}{\alpha_A} \qquad (12)$$

Meek assumed that for the streamer to propogate the space charge field must equal the applied field. This means $\alpha_A$ is a constant equal to $\alpha$ at the anode. The above equation can be written in this form:

$$\int_0^d \alpha(x)dx = K_1 = \log_e \frac{C_1 E_s}{\alpha_A} \qquad (13)$$

This equation is the equation of Schuman.[22] He specified that $K_1$ have the value of approximately 20 at atmospheric pressure and uniform field.

If the value of $K_1$ is evaluated from measured breakdown

voltages in non-uniform fields for various gap lengths, it is found that $K_i$ varies from about 10 to 45 as the gap varies from 0.1 to 10 centimeters. Since $\alpha$ varies greatly with field strength, values of breakdown using $K_i = 20$ will not be very far from the true values in the uniform field. Consequently, results are obtained using this criterion. In a non-uniform field, the assumption has little validity. The function that replaces $K_i$ should include factors that participate in the ionization process. The equation would read

$$n_A e^{\int_o^d \alpha(x)dx} = G(d, p, X_s, \mu, \%H_2O, \ldots) \qquad (14)$$

where G is the unknown function of gap length d, density p, field distribution $X_s(x)$, photo-ionization in the gap $\mu$, humidity $\%H_2O$, and other factors. Work in the area has shown that d and p are the dominant variables, so the other factors are neglected. The equation is:

$$n_A e^{\int_o^d \alpha(x)dx} = G(d,p) \qquad (15)$$

If the pressure is held constant, the equation may be re-written to be

$$\log_e (n_A) + \int_o^d \alpha(x)dx = g(d) = \log_e G(d,p_o) \qquad (16)$$

If the field is uniform, $\alpha$ is constant and

$$\log \alpha + \alpha d = g(d) \qquad (17)$$

Under these conditions, the values of g(d) can be calculated using breakdown values for different d in a uniform field. When g(d) is determined this way, the field distortion caused by the field is neglected. Since the distortion is also neglected when the equation is applied to the non-uniform field, the error will tend to compensate for itself to some extent.

This method could be used to calculate values of breakdown for any gas where the values of $\alpha$ near breakdown are known. However, these values are not yet known to sufficient accuracy to prive if the method is valid for many gases.[23]

The method just given was set forth by A. Pedersen, who claimed that it would hold for impulse waves. He states that the method is a semi-empirical quantitative breakdown criterion. He has correlated breakdown in uniform fields with that in non-uniform fields.

However, it is the feeling of this author that the method, being an extension of Meek's proposal for non-uniform fields, is subject to the same criticisms that can be leveled at Meek's original theory.[24]

Nothing regarding the matter of statistical time lags has been taken into account here. It has been shown that

these lags are of importance in dealing with impulse waves. It can be said that if this method assumes the presence of sufficient initiatory electrons at all times, it will probably give the lowest possible value of breakdown to be expected. The static uniform field case will also give this lower limit.

Although the theories accounting for the mechanisms of electrical breakdown of gases lend much to the understanding of the physical phenomena involved, it can be seen that in the design of his equipment, the engineer must rely on experimentally found limits in determining the insulation levels for that equipment. He also finds that the best way to evaluate his insulation system is by test and comparison. This is true because the theories are complex and hard to evaluate and that they require experimental data in their evaluation. The results of the theoretical calculations are limited in both application and accuracy.

# TEST PROCEDURES AND EQUIPMENT

## Gas Test Cell

### 1. Construction

The test cell used for this experiment was a cell especially designed for electrical tests on gases and is shown in Figure 1a. It is currently being used by several laboratories and industrial researchers. The cell was constructed by M. J. Seavy and Sons. It consists of two machined aluminum electrode holders clamped to a two inch inside diameter by eight inch long pyrex glass cylinder. The aluminum ends have provisions for admitting and sealing gases and for micrometer adjustments of the electrode gap. The internal volume of the cell, considering the displacement of the electrodes, is approximately 350 milliliters.

The electrode configuration used in the cell was in accordance with suggestions listed in an AIEE paper on standardization of testing procedures on gases.[25] It was intended that the suggested system A, consisting of a 3/4" diameter sphere and a 1-3/4" diameter grounded plane, be used. After testing had begun, it was discovered that the sphere was 1" instead of 3/4". The remainder of the testing was carried out using this system which was designated system A'. Both electrodes were made of brass of unknown composition.

# TEST CELL

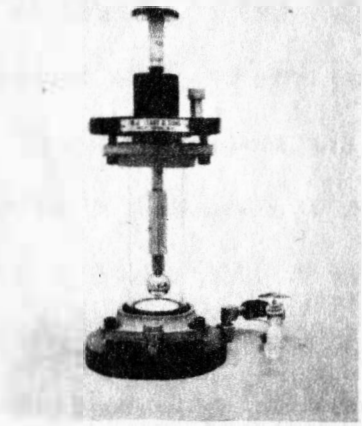

a

# IMPULSE GENERATOR

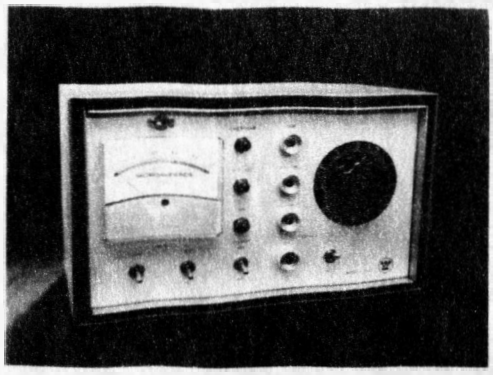

b

CONTROL CABINET

c

HIGH VOLTAGE UNIT

Fig. 1

2. Cleaning and Preparation for Testing

Between each set of tests run on the cell, the cell was given a standard cleaning. The cell was disassembled and the electrodes sanded with emery paper and polished with a rouge wheel. The electrodes and inside parts of the test cell were washed with laboratory glass cleaner and water. The parts were rinsed with distilled water and chemically pure acetone. The cell was reassembled and evacuated with a vacuum pump for at least 15-20 minutes. An oil seal type of pump was used which would exhaust to a pressure about one millimeter of mercury.

3. Filling the cell

The gas was transferred to the cell using the apparatus shown in Figure 2. The nitrogen used was obtained from a local supplier. The gas was water-pumped grade and was pure to about 99.6%.

The cell and flasks A and B were evacuated by the pump. Leveler tube C was raised so the silicone oil level came to the stopcock. Silicone oil was used to prevent gas contamination. The valves on the gas cylinder were adjusted so the gas bubbled slowly out of tube D through opening E. The gas was passed through dried KOH pellets to remove moisture in the gas. When sufficient evacuation had taken place, (approximately 10 minutes) stopcock F was closed. Stopcock H was opened very slightly and gas allowed to seep into

# GAS HANDLING EQUIPMENT

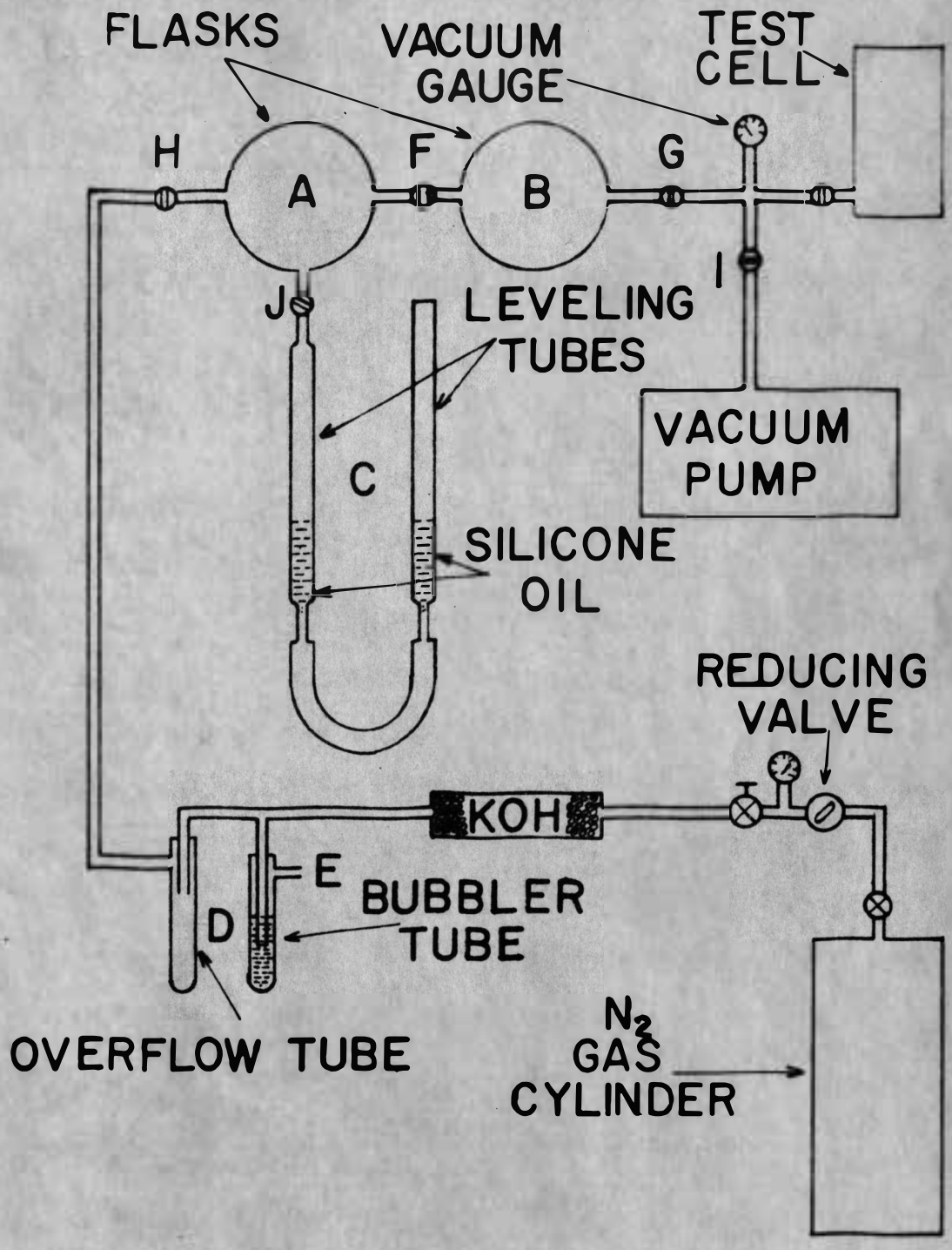


Fig. 2

flask A. Care was taken to insure bubbling continued in D while A was filled. When A was full, stopcocks G and H were closed and stopcock F was opened. Again stopcock H was opened slowly and flasks A and B were filled. Stopcocks H and I were closed and G was opened, H was opened slowly and the cell was allowed to finish filling.

When the cell was filled with gas, the electrode gap was closed until an ohmmeter indicated zero gap. The micrometer setting was noted and the gap opened to one-half inch.

Stopcock H was closed, I was opened and the system again evacuated. The system was refilled as before. Two evacuations and fillings were used to insure the purity of the sample tested. Stopcock J was then opened and H closed. Temperature and atmospheric pressure readings were taken in the room. The pressure in the cell was adjusted using the leveler tube to give a standard condition of 80°F and 28.35 inches of mercury, this being average temperature and pressure at test location. The cell stopcock was closed and the cell was ready for testing.

D.C. Voltage Tests

1. Test equipment

The D.C. voltages were obtained from a power supply supplied by the Kilo-volt Corporation. It consisted of a voltage doubler circuit using an auto-transformer input.

The maximum output was 120 K.V. at 5 ma. The rated ripple was less than 0.5% at rated output. The testing circuit arrangement was as shown in Figure 3. The voltage at the cell was measured by a voltage divider. The divider resistor was a precision 120 megohm resistor constructed by the author of 31 resistors connected in series enclosed in a glass tube filled with transil oil. Measurements were taken across a one megohm 1% resistor at the ground end using a D.C. VTVM of 1/2% accuracy. It was found, using the voltage divider, that the D.C. breakdown voltages were at a higher voltage than the A.C. This could not possibly be so. The divider was checked against a set of 6.25 cm sphere gaps. The check showed that the divider relationship was not accurate.

Under high voltage D.C., the divider resistance dropped to a value of about 1.08 megohms due probably to the shunting of resistors by the resistivity of the oil. This problem was not investigated due to lack of time. The sphere gap calibration of the divider was used to obtain the values of D.C. voltage indicated in this report.

At voltage levels needed for this experiment, the corona leakages from the circuit were not measurable although a trace was present.

2. Conduction of D.C. tests

The tests were conducted by raising the voltage

# D-C TEST CIRCUIT & SET

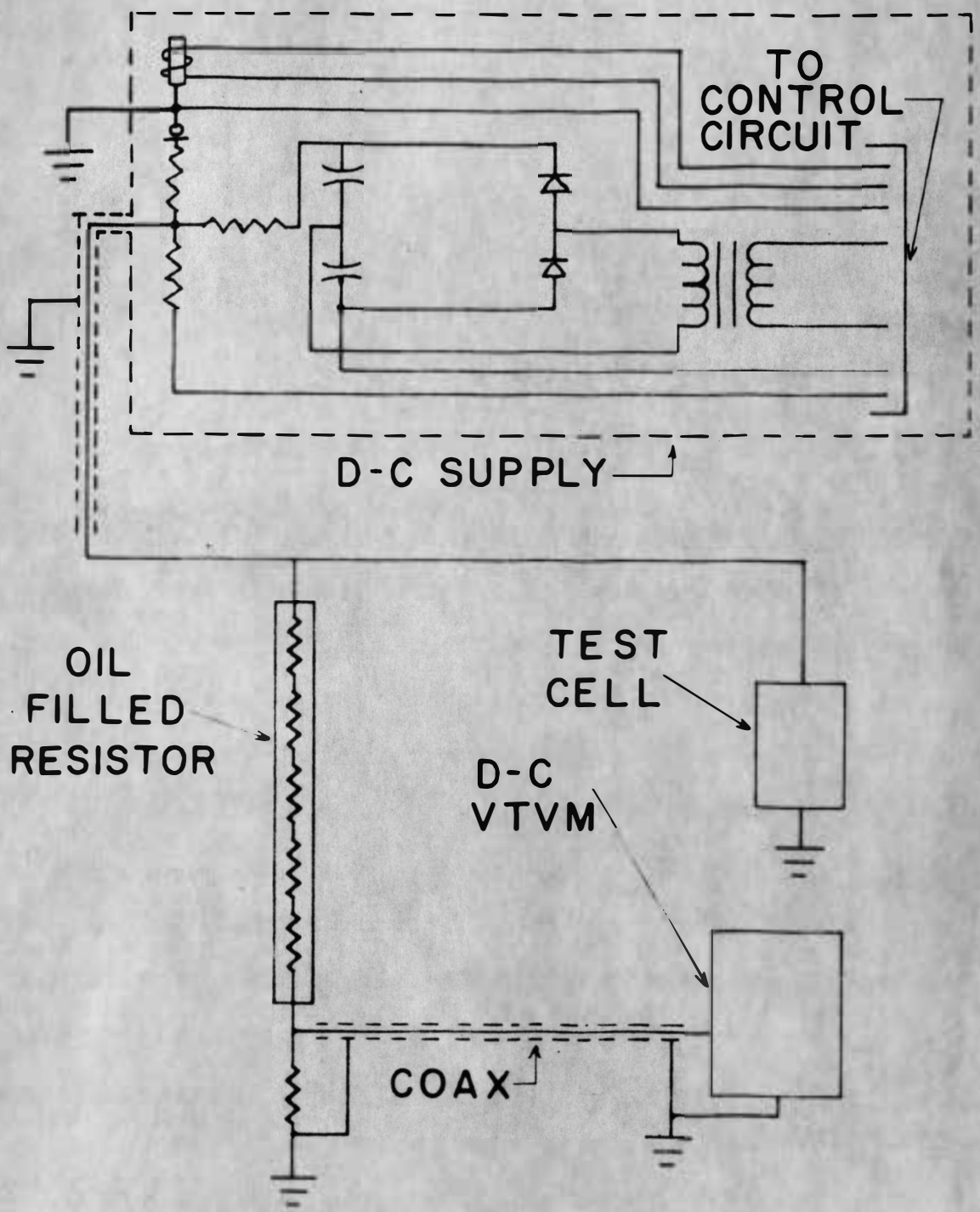


Fig. 3

manually at a rate of approximately 1.2 K.V. per second until breakdown occurred. After a one minute rest, the test was repeated until five trials had been made. The voltage was then raised to approximately two-thirds of the apparent breakdown point. It was raised 1.2 K.V. at the end of each minute until a discharge occurred. This was repeated four more times. The cell was then removed and another identical cell placed on the test set and the above process repeated for it.

60 Cycle Voltage Tests

A 75 K.V., 60 cycle, General Electric testing transformer was the 60 cycle source. The set was corona free up to its top rating. The output voltage was measured by high impedance meter connected to a voltmeter coil that is an integral part of the test transformer set.

The voltage was applied at a rate of approximately one K.V. per second by manually adjusting a variable autotransformer until breakdown occurred. After a rest of one minute, the test was repeated until five trials had been made. The voltage was then raised to approximately two-thirds of apparent flashover point. At intervals of one minute, the voltage was raised one K.V. until breakdown occurred. This was done five times. The cell was then removed and another identical cell was tested following the above procedure.

## Impulse Voltage Tests

### 1. Test Set

The impulse waves were obtained from a portable impulse generator built by Westinghouse rated at 125 K.V. The unit is shown in Figure 1b and c. The control cabinet contained a voltmeter that read voltage applied to the first capacitor in the generator. The generator used a Marx, parallel charge-series discharge of capacitors circuit, so the voltage at the first capacitor was, after a time had elapsed, essentially the voltage on all capacitors, three in this unit. Upon triggering by a mechanical arm which shorted the first set of sphere gaps, the voltage at the output terminal was three times the voltage read on the meter, less drops across internal air gaps used to put capacitors in series.[26]

### 2. Wave shaping circuit

The wave shaping circuit is shown in Figure 4. $R_1$ was less than $R_2$ so $C_1$ charged to a peak voltage through $R_1$ and discharged through $R_2$. $R_2$ was the total resistance from top of $C_1$ to ground. $R_s$ was series resistor across which the oscilloscope voltage was developed. The voltage at the oscilloscope was then $R_s/R_2$ of the voltage at the cell. The oscilloscope used was a Tektronix Type 507 with a maximum applied voltage of 3000 volts and a maximum

# IMPULSE SET & CIRCUIT

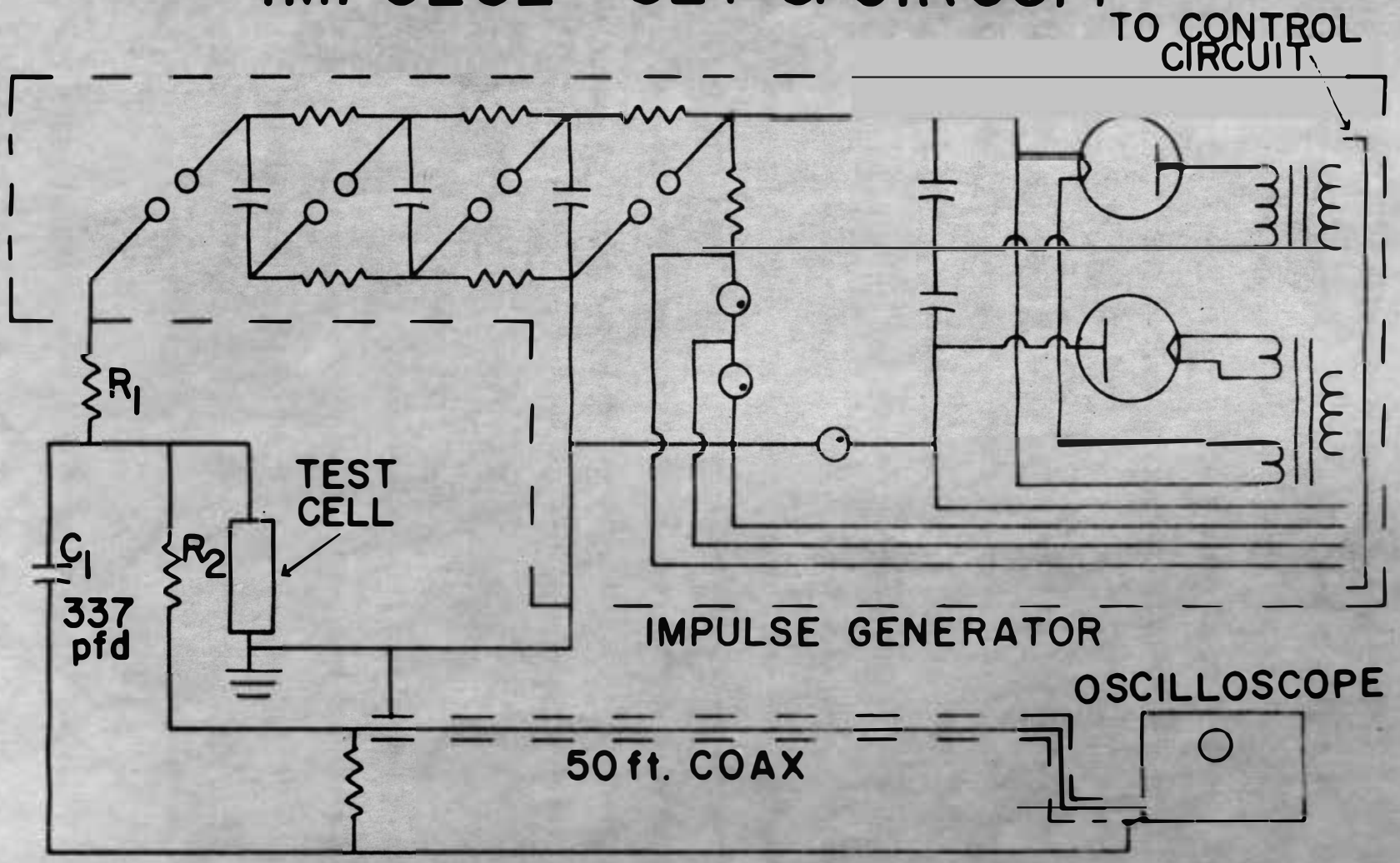


Fig. 4

writing speed of $20 \times 10^{-9}$ seconds/centimeter. The oscilloscope had an input impedance of 72 ohms, so a 40 foot 75 ohm coaxial cable was used to connect the oscilloscope to the divider. A 75 ohm non-inductive resistor was used as series resistor at the divider to terminate the cable. $R_s$ was the parallel combination of 72 and 75 ohms for most experiments.

The wave shape used was that specified by AIEE Standards #4, 1953. The front of wave rose to crest in time $t_1$ and dropped back to one-half crest in time $t_2$, both measured from time zero of the wave. In the present experiment, times $t_1$ and $t_2$ were varied by circuit adjustment. This was accomplished by holding capacitor $C_1$ constant and changing the values of $R_1$ and $R_2$. A theoretical analysis of the wave shaping circuit is given in appendix two. From this analysis, $t_1$ and $t_2$ could be determined knowing values of $R_1$, $R_2$ and $C_1$. Presumably, values of $R_1$ and $R_2$ could be found knowing $t_1$, $t_2$ and $C_1$.

3. Wave shape adjustment

This procedure proved to be mathematically difficult. So the times $t_1$ and $t_2$ were determined experimentally. $R_1$ and $R_2$ were varied and the resulting changes in $t_1$ and $t_2$ were noted with the oscilloscope. $t_1$ depended mostly on $R_1$ and $t_2$ depended mostly on $R_2$. When the wave looked correct on the oscilloscope, a picture of the wave was taken using a Polaroid camera mounted on the oscillo-

scope. Measurements of the wave were taken on the picture to insure that proper times had been attained. Pictures were taken of all waves used and are shown in Figures 5c and d through 8. Pictures were taken of both positive and negative 1-1/2 x 40 waves as shown in Figure 6. The two were seen to be identical except for polarity, so pictures were taken only of the positive waves for the remainder of the waves used.

4. Equipment for long tail waves

Since large values of $R_2$ were needed for waves with very long tails, the voltage across $R_s$ became small. The type 507 oscilloscope needed a peak voltage of at least 50 volts to operate; therefore, Tektronix type 545A oscilloscope was used on these waves. The 545A had an input impedance of one megohm, a maximum input voltage of 120 volts and maximum writing speed of one microsecond/centimeter. The cable was terminated at the oscilloscope end with a 75 ohm non-inductive resistor whenever the 545A was used.

The resistors used in the wave shaping circuit were card resistors wire wound to be non-inductive, except for waves with very long tails, where regular wire-wound power resistors were used. The divider using these regular power resistors was checked by placing a non-inductive resistor voltage divider in parallel with it. The two dividers gave identical results indicating the inductance of the power

# FRONT OF WAVE OSCILLATIONS

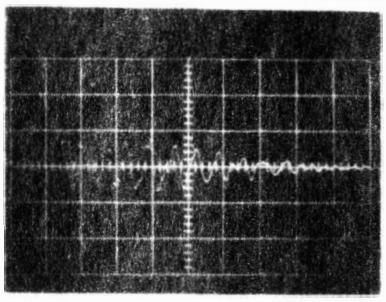

a

VERTICAL
1375 kv./cm.

SWEEP RATE
0.1 μsec./cm.

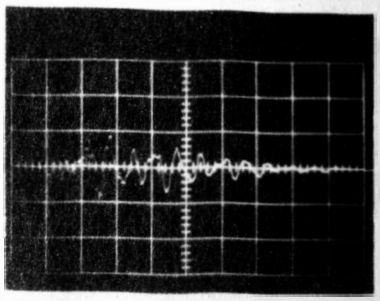

b

VERTICAL
1375 kv./cm.

SWEEP RATE
0.1 μsec./cm.

# 0.5x10 WAVE - POSITIVE

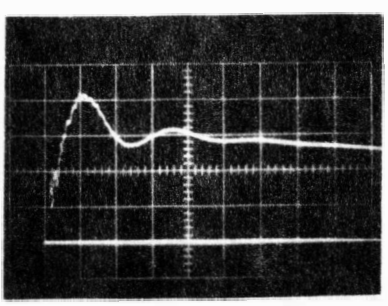

c

VERTICAL
9.74 kv./cm.

SWEEP RATE
0.5 μsec./cm

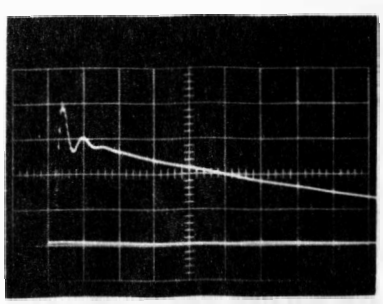

d

VERTICAL
9.74 kv./cm.

SWEEP RATE
2 μsec./cm

Fig. 5

# 1.5 x 40 WAVE - POSITIVE

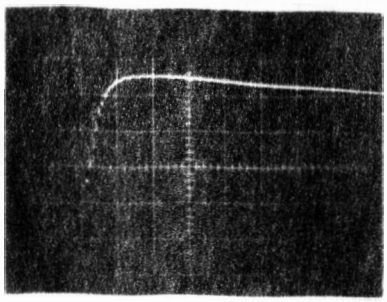

a
VERTICAL
6.62 kv/cm

SWEEP RATE
1.0 μsec/cm

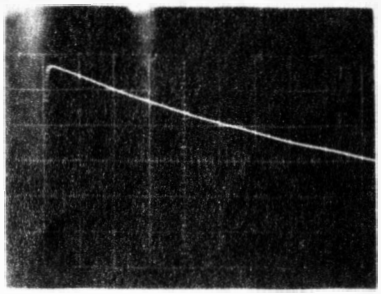

b
VERTICAL
6.62 kv/cm

SWEEP RATE
5 μsec/cm

# 1.5 x 40 WAVE - NEGATIVE

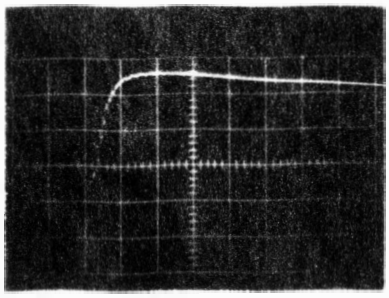

c
VERTICAL
6.62 kv/cm

SWEEP RATE
1.0 μsec/cm

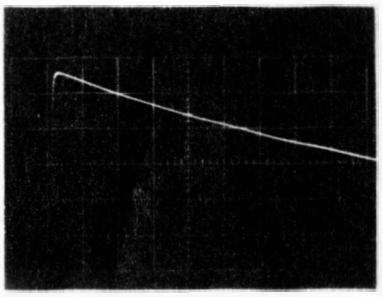

d
VERTICAL
6.62 kv/cm

SWEEP RATE
5 μsec/cm

Fig. 6

# 5 x 100 WAVE - POSITIVE

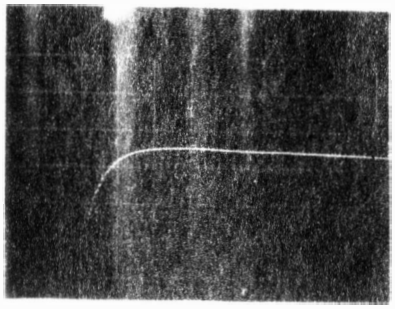

a

VERTICAL
10.88 kv/cm

SWEEP RATE
2 μsec/cm

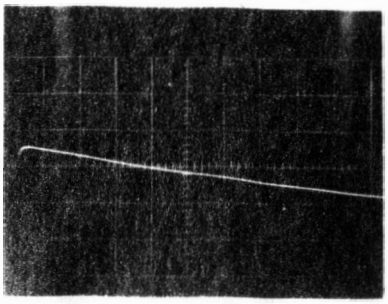

b

VERTICAL
10.88 kv/cm

SWEEP RATE
10 μsec/cm

# 50 x 1000 WAVE - POSITIVE

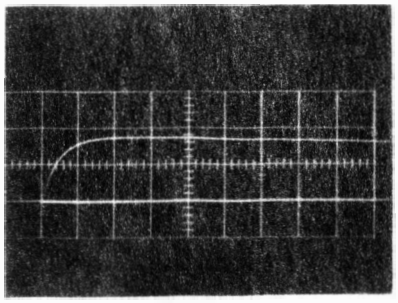

c

VERTICAL
16.37 kv/cm

SWEEP RATE
20 μsec/cm

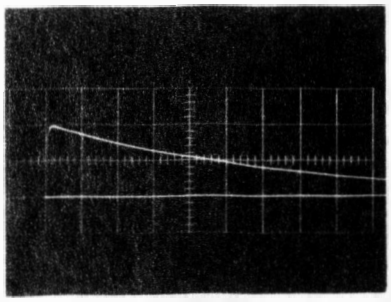

d

VERTICAL
16.37 kv/cm

SWEEP RATE
200 μsec/cm

Fig. 7

resistors was not affecting their results.

5. Voltage measurements

The voltage present at the cell was measured using the oscilloscope deflection and the voltage divider circuit. The standard wave, 1-1/2 x 40 microseconds, was measured with a set of 6.25 cm. sphere gaps. The generator output was controlled using the meter on the control panel. The output voltage of the set was determined using the sphere gaps as prescribed by AIEE Standards #4, 1953, using the correction factors for density and temperature. The 50% arcing point was found in terms of the control panel meter setting. The calibration curve of voltage versus panel meter settings is given in Figure 9. The output voltage calibration of the generator by means of the sphere gaps was compared to the voltage divider readings and the two were found to compare within the specified 3% of the standards.

When the output voltage of the divider circuit was observed on the scope using large $R_2$, high oscillations were noticed at the very front of the wave as shown in Figure 5a and b. Measuring the peaks of these oscillations on the picture indicated that, if these oscillations were present at the cell, their magnitude was on the order of a megavolt. Different circuit configurations and test equipment positions were found to have no effect on these oscil-

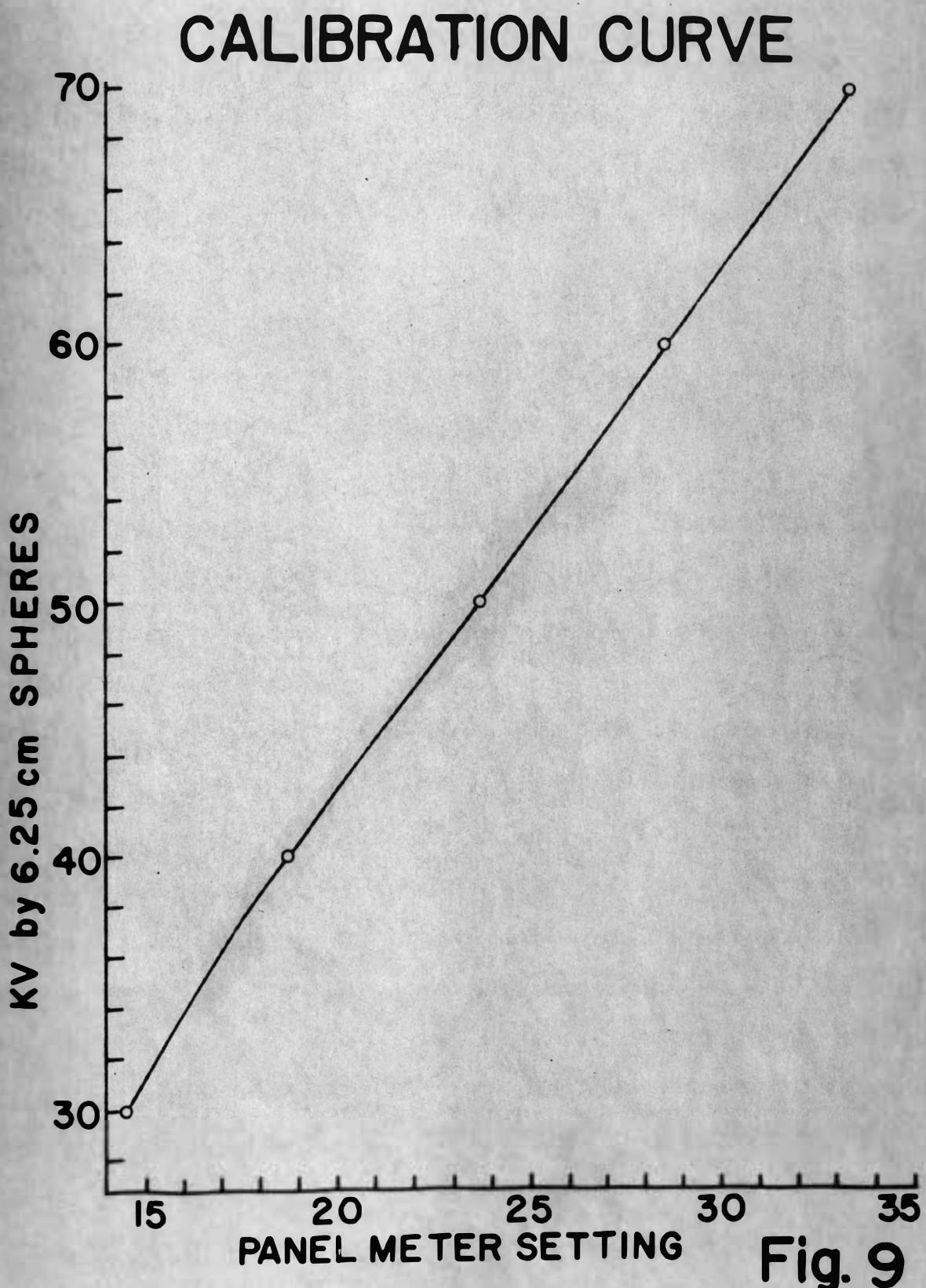
CALIBRATION CURVE
70
60
50
40
30
KV by 6.25 cm SPHERES
15
20
25
30
35
PANEL METER SETTING

Fig. 9

lations. Using two oscilloscopes, one directly across the cell and the other on the divider, it was found that the oscillations were not present at the cell. The oscillations were possibly caused by ringing in the cable and its associated resistors. These oscillations on the front of wave were ignored in the rest of the work.

6. Test Procedures

The impulse voltages were started at a level that caused breakdown on less than 10% of the trials. This magnitude of wave was then applied 10 times with a 30 second rest between applications. The voltage was then raised one unit on the panel meter and the wave was applied 10 times at this level after which the level was increased one more unit. This process was repeated until a level was reached where the gap broke down on more than 90% of the trials. The cell was then rested 5 minutes. Ten more trials were then taken at the same level just used (90%+). The level was decreased one unit and ten more trials run. The voltage was decreased in this manner until the gap flashed over less than 10% of the time. The cell was again rested for five minutes. Then a repeat of the first set of trials was run. This meant that at each voltage level, the cell was pulsed 30 times. A second cell, essentially identical to the first was placed on the circuit and it was pulsed 30 times for each level exactly as the first had been. A sam-

ple of this method of recording is shown in Figure 10.

7. Reduction of data to Kilovolts

During the time the cells were under test, the applied wave was observed with the oscilloscope. The peak millimeter height of each wave was recorded. The voltage being applied was determined by knowledge of the resistance divider values. A plot of millimeter height observed versus panel meter setting was made as shown in Figure 11. Using this graph, voltage level settings were converted to peak K.V., and tables made of per cent breakdown versus peak voltage applied were made. These values are shown in tables 4 through 8 in appendix one.

Source of Ionization

It was first proposed that the tests would be run using only background irradiation. It was found that the breakdown pattern was so erratic that 100% breakdown could not be achieved with the impulse generator even at levels close to 100 K.V. crest, 1-1/2 x 40 wave, for a 1/2" gap setting. So a source of weak external ionization was used. This consisted of a millicurie of radium placed in a lead can 18 inches from the electrode center line and 1.37 inches of lead in the can. This gave a gamma ray count of approximately 3300 counts/sec at the electrodes without the glass wall of the test cell present. The count of natural back-

# METHOD OF RECORDING DATA

## 50×1000 usec WAVE - POSITIVE POLARITY

CELL no.1

| panel meter setting | trials | oscilloscope deflections |
|---|---|---|
| | cycle no.1 | |
| 15.0 | o o x o o o o o o o | 20.5⁻ mm |
| 15.5 | o o x o o o x x o o | 21.0⁺ mm |
| 16.0 | x x o x o x o x o x | 22.0⁻ mm |
| 16.5 | x o x o o x x x o o | 22.0⁺ mm |
| 17.0 | x x x x x o o x x x | 23.0 mm |
| 17.5 | x x x o x x x o x o | 23.5⁺ mm |
| 18.0 | x x x x x x x x x x | |
| | cycle no.2 | |
| 18.0 | x x x x x x x x x x | |
| 17.5 | x x o x x x o o x x | |
| 17.0 | o x o o o x x x o o | 23.0 mm |
| 16.5 | o x x o x x o o o o | 22.0⁺ mm |
| 16.0 | o o o o o o x o o o | 21.5 mm |
| 15.5 | o o o o o o x o o o o | 21.0⁻ mm |
| 15.0 | o o o o o o x o o o o | 20.0⁺ mm |
| | cycle no.3 | |
| 15.0 | o o o o o o o o o o | 22.0⁻ mm |
| 15.5 | o o o o o o o o o x | 21.0 mm |
| 16.0 | o o o x o o o x o o | 21.5 mm |
| 16.5 | x o o x x o x x o x | 22.0⁺ mm |
| 17.0 | o x x o o x o x o o | 23.0⁻ mm |
| 17.5 | x x x x o o x o x o | 23.5 mm |
| 18.0 | x x x x o x x x x x | 24.0⁺ mm |

x = breakdown
o = no breakdown

Fig.10

# EXAMPLE CONVERSION CURVE

## Panel Meter To mm Deflection

| cycle | panel meter setting | | | | | | |
|---|---|---|---|---|---|---|---|
| | 15.0 | 15.5 | 16.0 | 16.5 | 17.0 | 17.5 | 18.0 |
| 1st | 20.5 | 21.0 | 22.0 | 22.0 | 23.0 | 23.5 | |
| 2nd | 20.0 | 21.0 | 21.5 | 22.0 | 23.0 | | |
| 3rd | 20.0 | 21.0 | 21.5 | 22.0 | 23.0 | 23.5 | 24.0 |
| 4th | 20.0 | 21.0 | 21.5 | 22.0 | 22.5 | 23.0 | 24.0 |
| 5th | 20.0 | 21.0 | 21.5 | 22.0 | 22.5 | 23.5 | 24.0 |
| 6th | 20.5 | 21.0 | 21.5 | 22.0 | 23.0 | 23.5 | 24.0 |

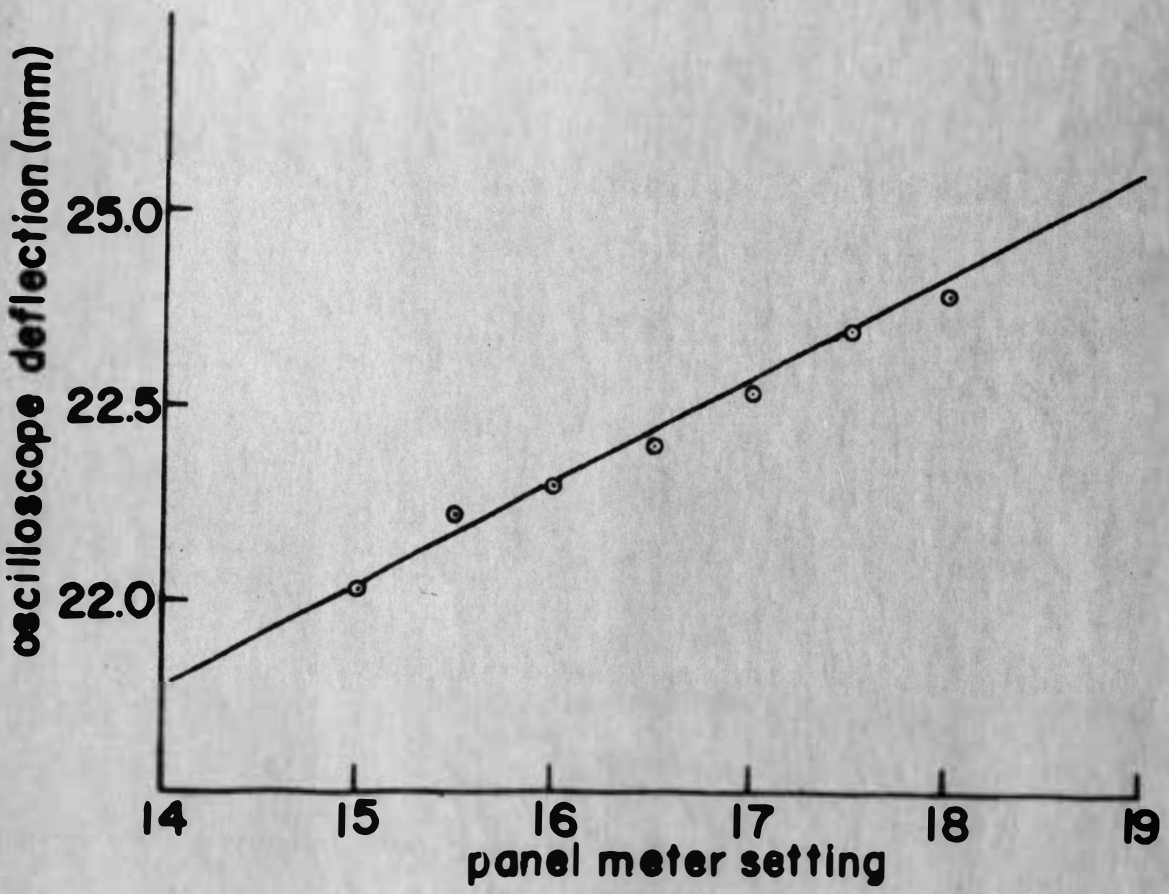


Fig. 11

ground at this point was 84 counts per second. It was assumed that ionization in the cell was primarily due to low energy gamma rays since beta rays would not penetrate the pyrex test cell walls. Very high energy gammas are scarce and have a lower probability of ionization. The gamma counts were taken over the energy range from 20 Kev to 1.13 Mev. As function of energy, it can be seen in Figures 12 and 13 that high energy gammas are few in number relative to lower energy rays. The effect of the glass walls of the test cell on the count can be seen in Figure 14. Here four glass walls were present between the source and the counter crystal. The effect of one glass wall on the count was to reduce the count by about 80 to 100 counts per second. This intensity of irradiation was used throughout the tests taken.

# GAMMA RAY COUNT

count of laboratory background
as a function of gamma ray energy

count time 60 minutes

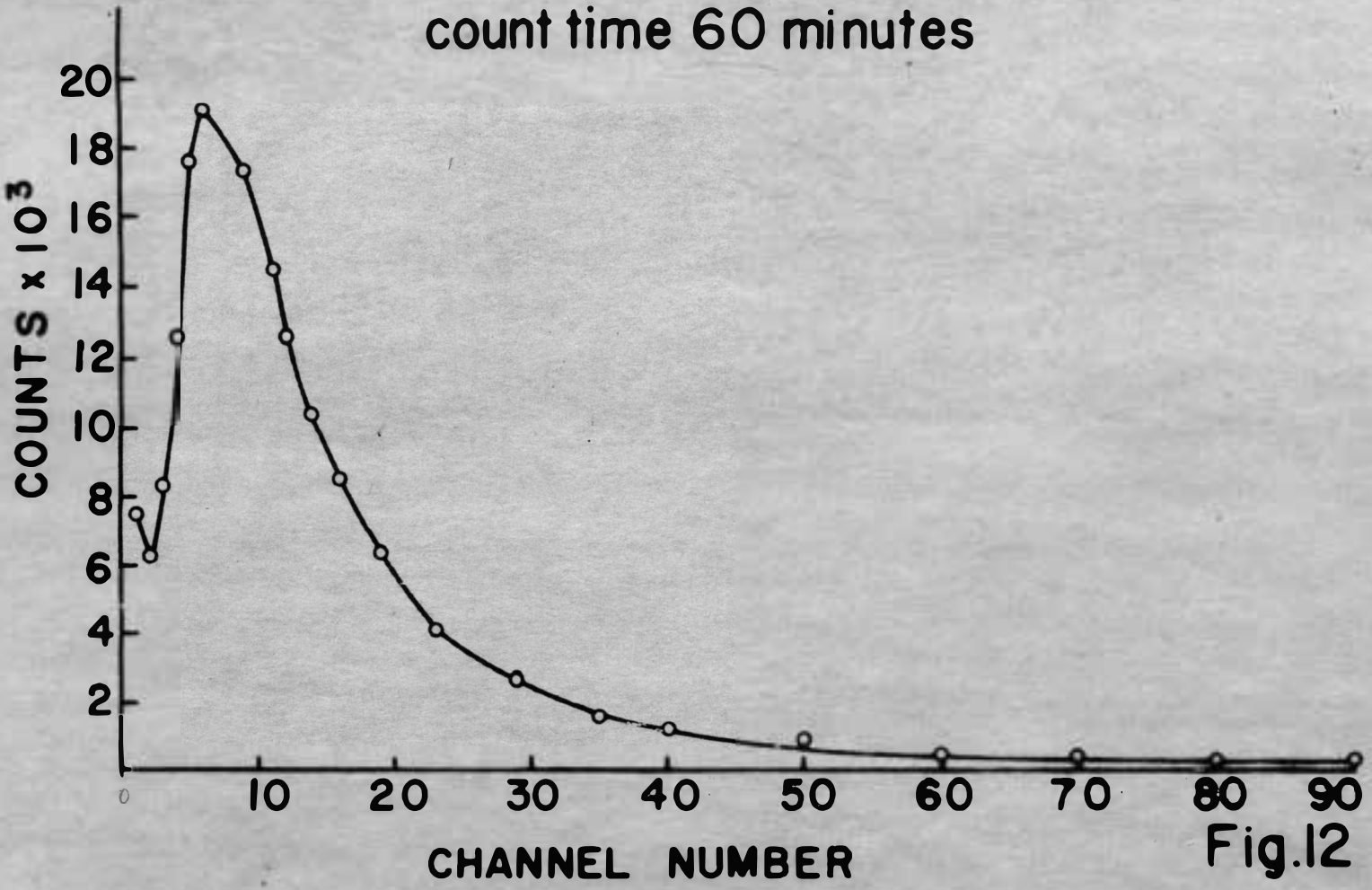


Fig.12

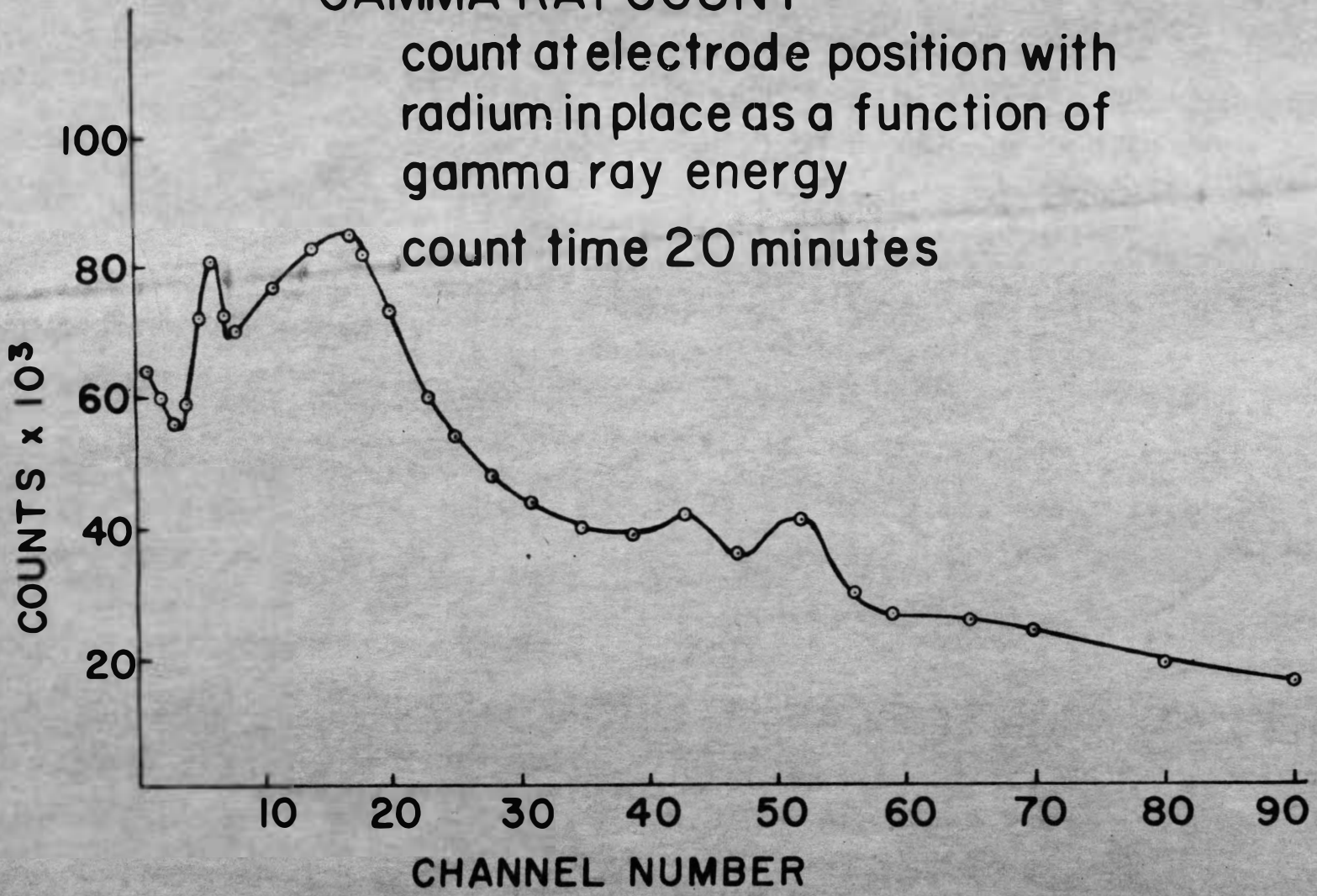
GAMMA RAY COUNT
count at electrode position with radium in place as a function of gamma ray energy
count time 20 minutes
COUNTS x 10³
100
80
60
40
20
10
20
30
40
50
60
70
80
90
CHANNEL NUMBER

Fig.13

# GAMMA RAY COUNT

count at electrode position with radium in place and shielded by 2 glass cylinders as a function of gamma ray energy

count time 20 minutes

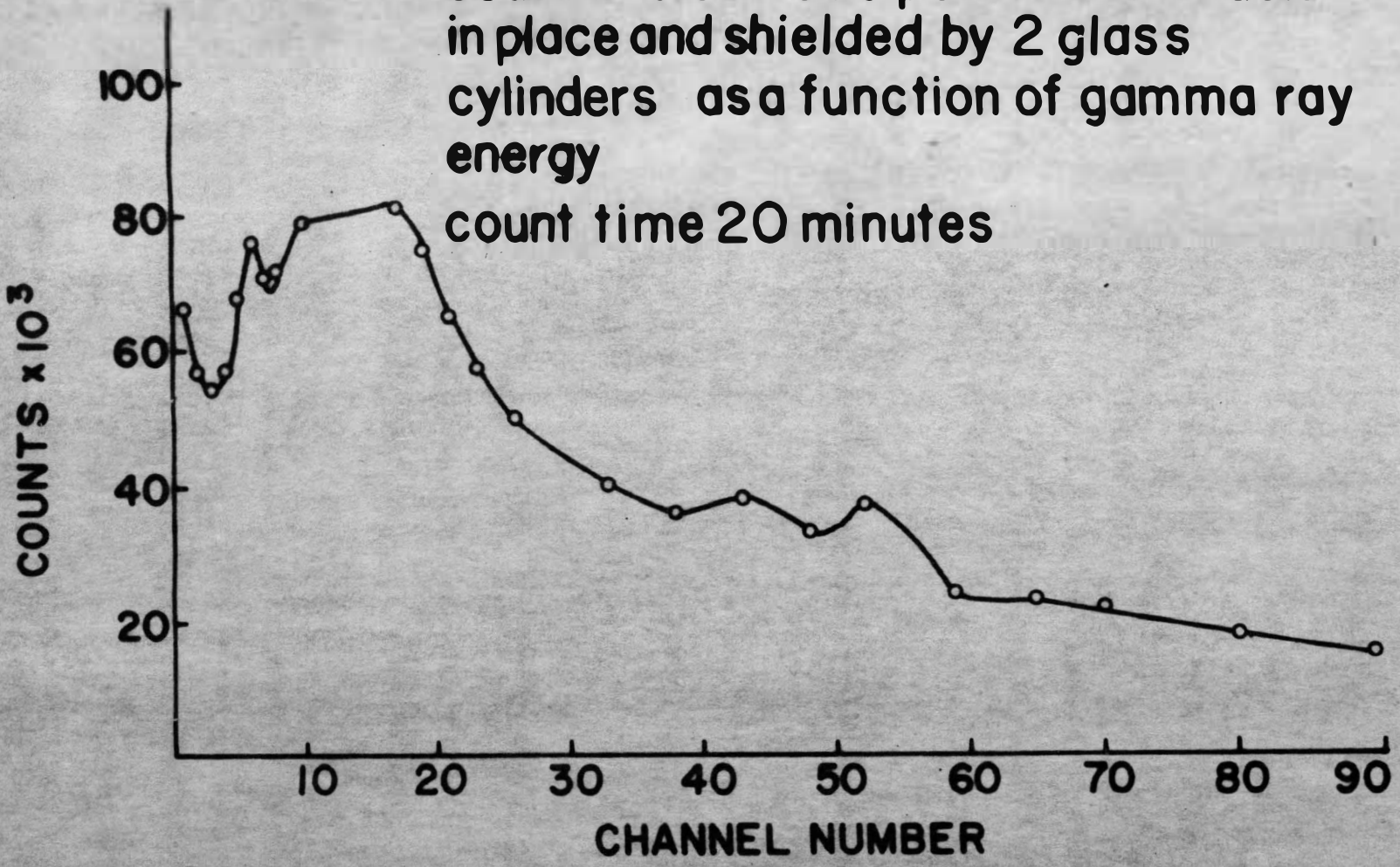


Fig. 14

# DISCUSSION OF RESULTS

## Test Results

The percentage of breakdowns versus the applied voltage for the different waves are shown in Figures 15 through 20. The shape of each of these curves can be seen to be in the general form of a probability distribution curve. This indicates that the relationship between per cent breakdown and applied voltage is statistical in nature.

The percentage breakdown curve shown in Figure 20 for the 550 x 9000 microsecond voltage wave, negative polarity, has some scattered data points. The data points rise until about 60 K.V. and start dropping in percentage from 80% to 50% at about 67 K.V. before rising back to 100% breakdown at 74 K.V. This dip shown in the data points was ignored when the curve was drawn. The 60 K.V. percentage is the result of 140 trials whereas the points above 60 K.V. are the result of only 20-40 trials. On several of the cycles, the 60 K.V. voltage level caused 100% breakdown, so higher levels were not taken. On the cycles that weren't breaking down 100% at 60 K.V., voltage levels higher broke down as shown by the data plots. The assumed points plotted were obtained using the assumption that cycles which gave 100% breakdown at 60 K.V. also broke down 100% at all higher levels even though the points were not tried. The result-

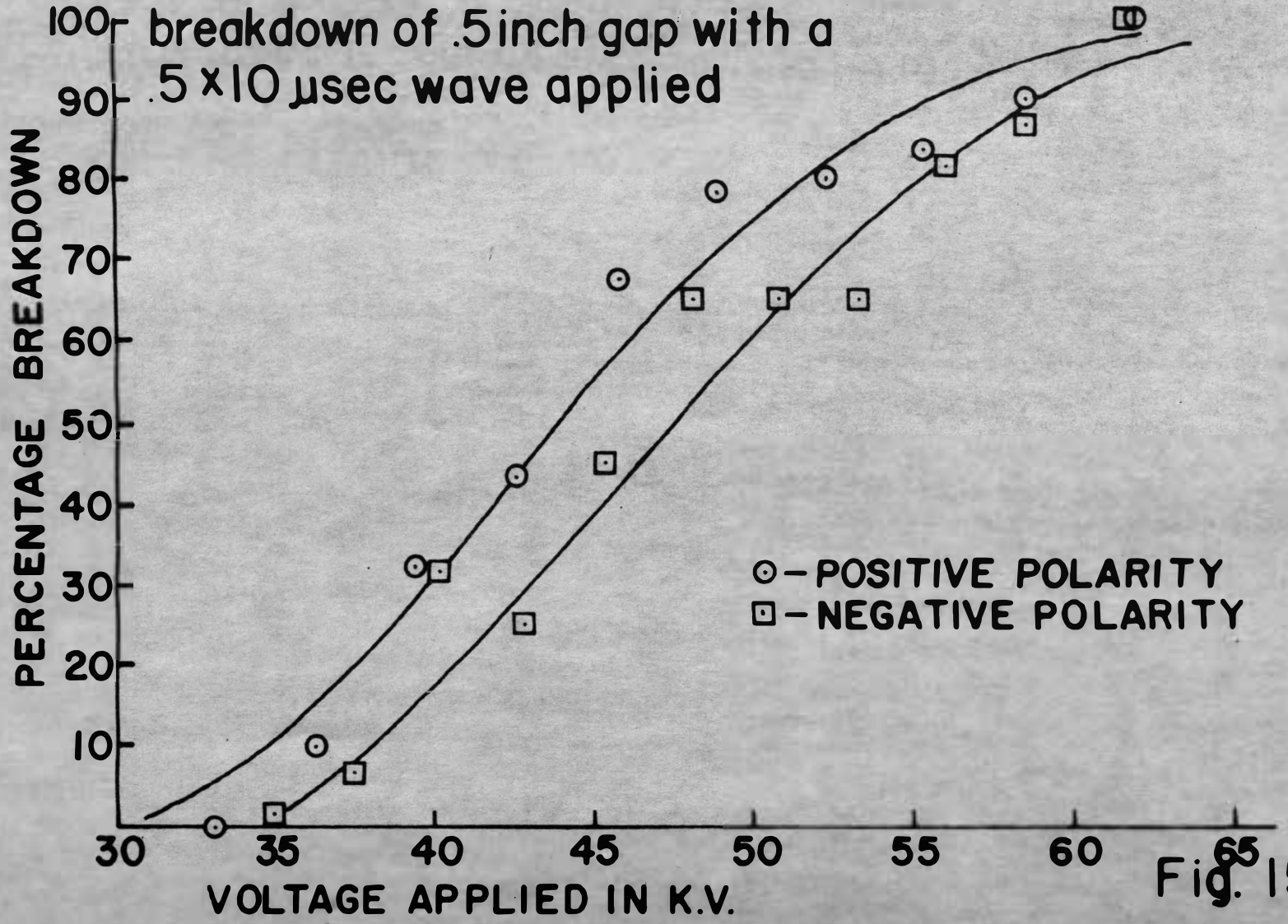
PERCENTAGE BREAKDOWN VERSUS VOLTAGE
breakdown of .5 inch gap with a
.5 x 10 µsec wave applied
PERCENTAGE BREAKDOWN
100
90
80
70
60
50
40
30
20
10
30
35
40
45
50
55
60
65
VOLTAGE APPLIED IN K.V.
⊙ - POSITIVE POLARITY
⊡ - NEGATIVE POLARITY

Fig. 15

# PERCENTAGE BREAKDOWN VERSUS VOLTAGE

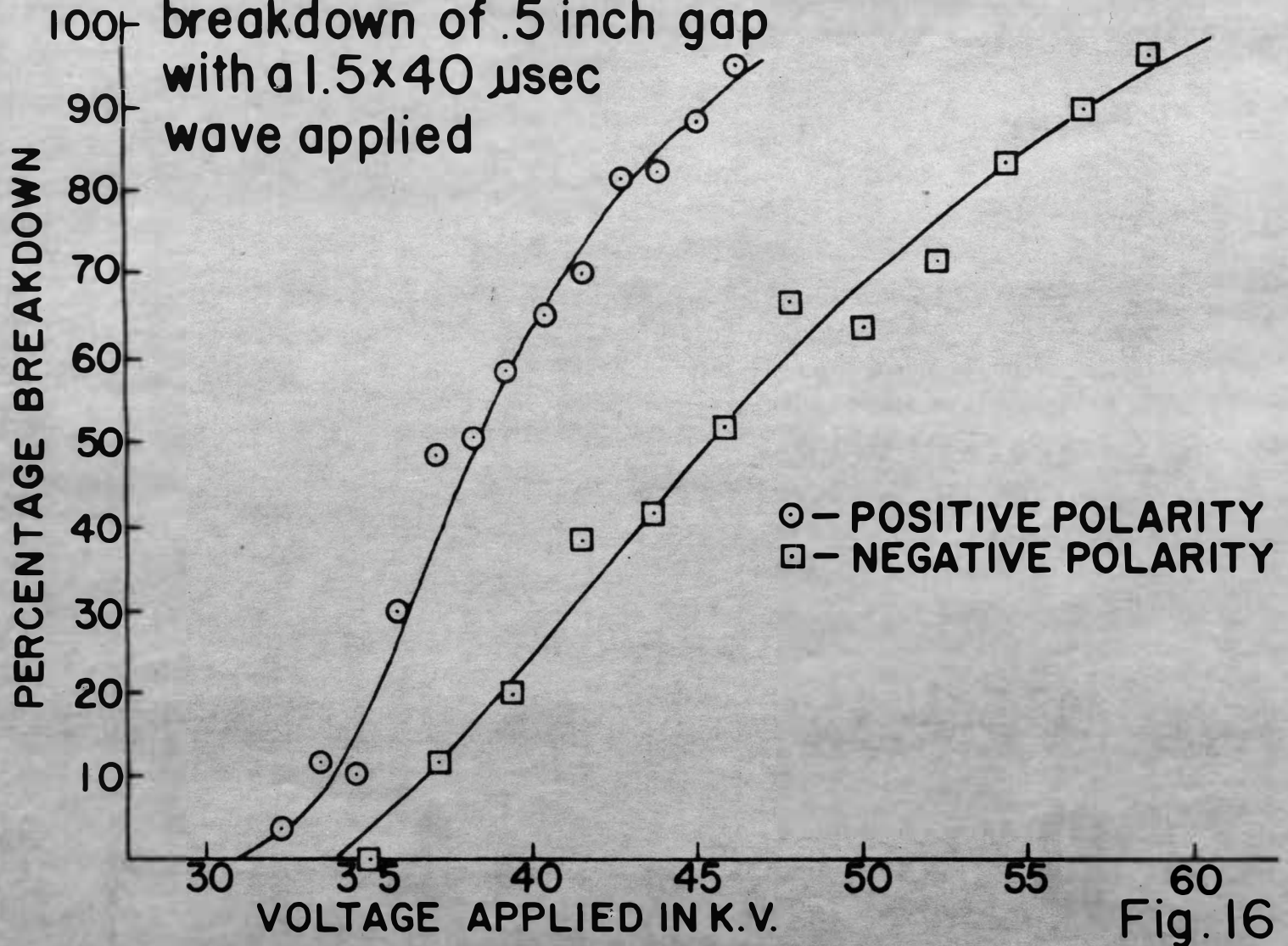


Fig. 16

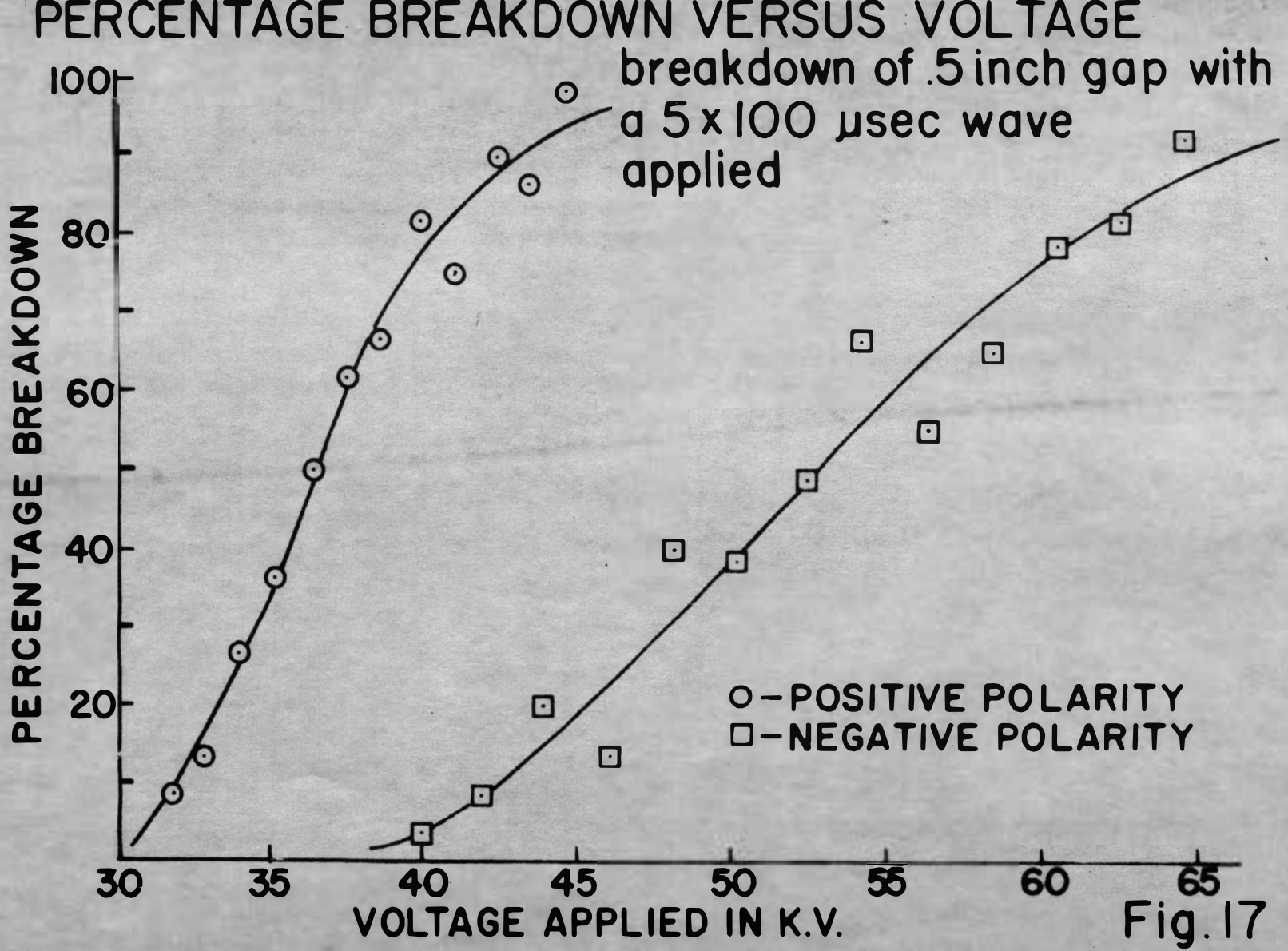
PERCENTAGE BREAKDOWN VERSUS VOLTAGE
breakdown of .5 inch gap with a 5 x 100 μsec wave applied
PERCENTAGE BREAKDOWN
100
80
60
40
20
30
35
40
45
50
55
60
65
VOLTAGE APPLIED IN K.V.
O-POSITIVE POLARITY
□-NEGATIVE POLARITY

Fig. 17

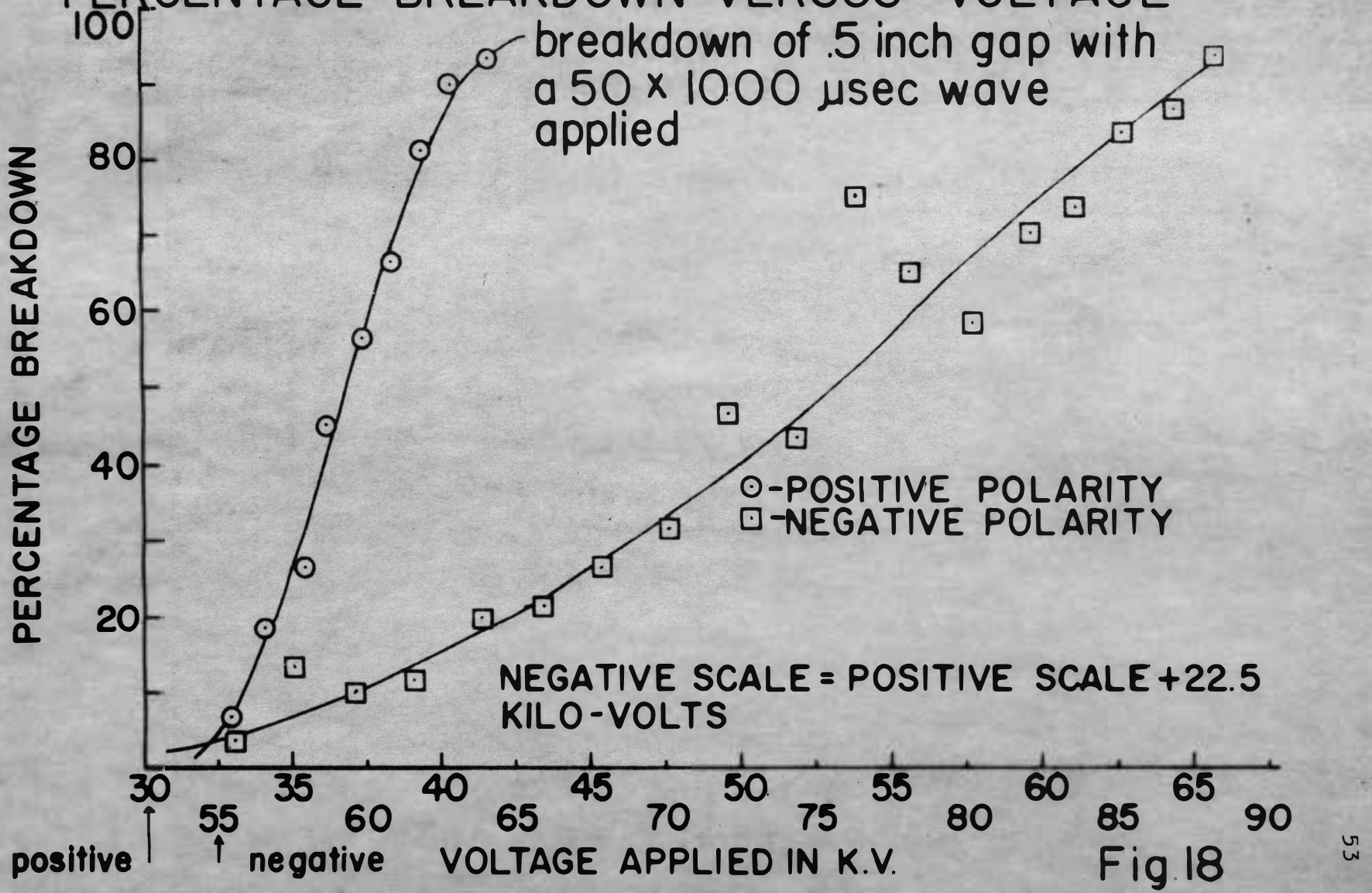
PERCENTAGE BREAKDOWN VERSUS VOLTAGE
breakdown of .5 inch gap with a 50 x 1000 µsec wave applied
PERCENTAGE BREAKDOWN
100
80
60
40
20
⊙-POSITIVE POLARITY
⊡-NEGATIVE POLARITY
NEGATIVE SCALE = POSITIVE SCALE + 22.5 KILO-VOLTS
30
35
40
45
50
55
60
65
55
60
65
70
75
80
85
90
positive
negative
VOLTAGE APPLIED IN K.V.

Fig 18

# PERCENTAGE BREAKDOWN VERSUS VOLTAGE

breakdown of .5inch gap with a 550 x 9000 μsec wave applied

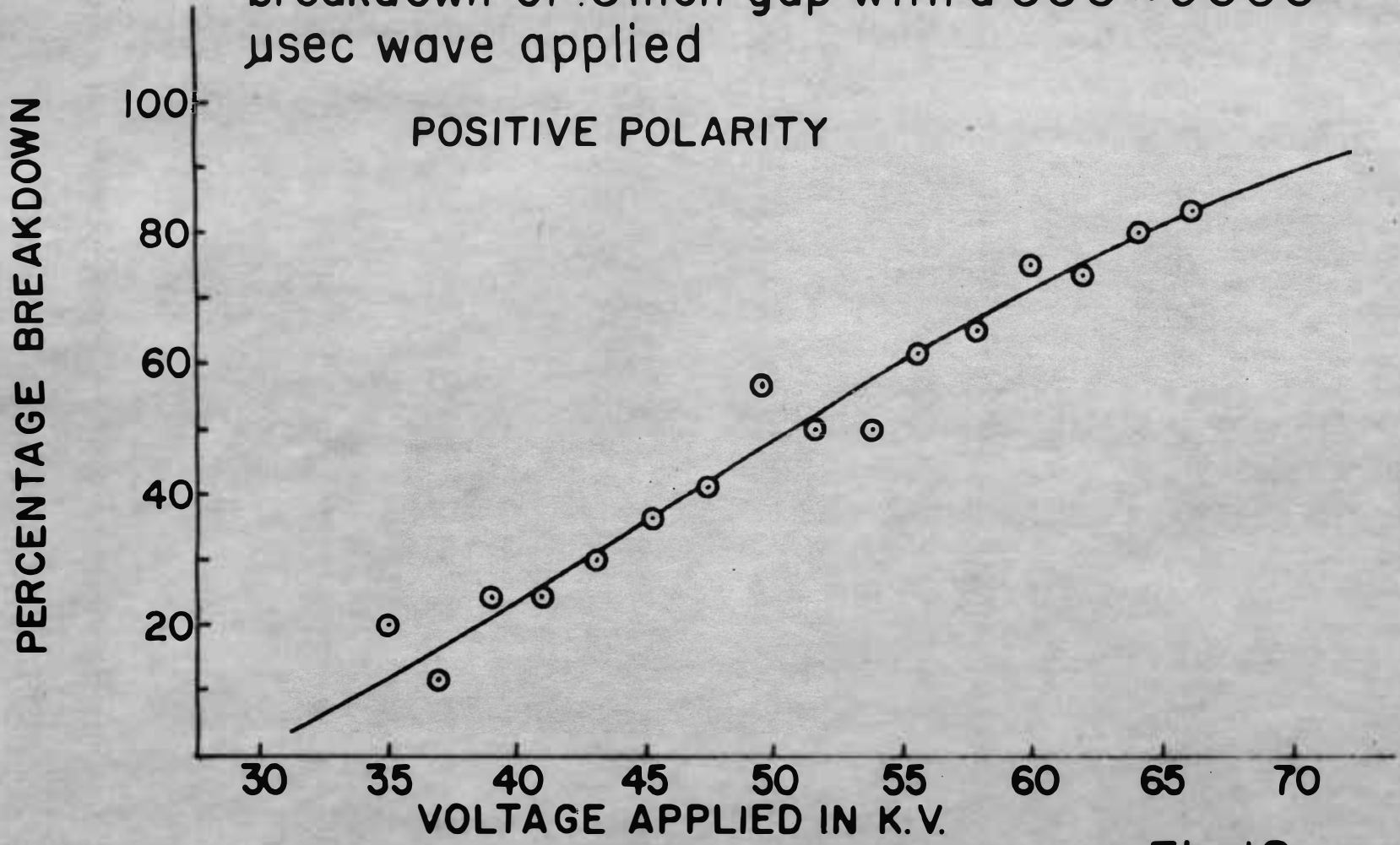


Fig.19

# PERCENTAGE BREAKDOWN VERSUS VOLTAGE

breakdown of .5 inch gap with a 550 x 9000 μsec wave applied

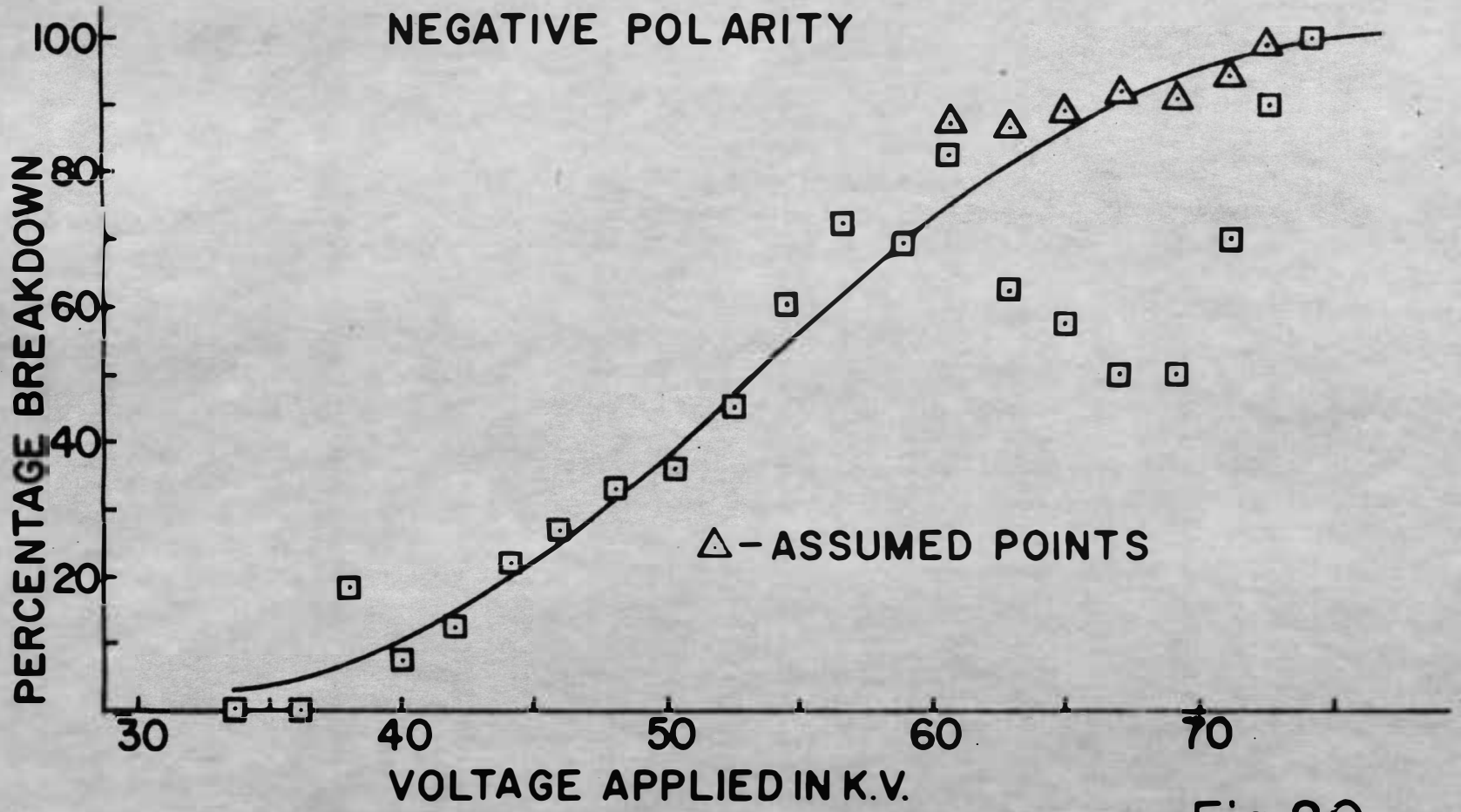


Fig. 20

ing curve is similiar to others and is taken to be correct for that reason.

It was found that the 60 cycle A.C. peak and the D.C. breakdown voltages of the gap were essentially the same. The difference was only 0.6%.

The plots of per cent breakdown voltage versus time to crest of the different applied voltage waves are shown in Figures 21 and 22. The 10%, 50%, and 90% breakdown voltage values were plotted for each wave and both polarities to show the spread of values. Both positive and negative polarity seem to follow the same general trend. The negative does rise to higher values of voltage at lower times than the positive polarity waves. The point where the positive polarity values begin to drop back down in voltage was not found due to lack of time and limits of the equipment. Figure 8 shows that the tail of the long wave is choppy. This was caused by the inability of the generator to keep the arcs between the internal spheres from quenching. The problem might have been remedied by using a generator of greater internal capacity.

It could be assumed that the positive polarity would be of the same general shape as the negative plot and would, therefore, soon decline to lower breakdown values. Further tests would be needed to verify this assumption.

# PERCENTAGE BREAKDOWN VOLTAGE AS A FUNCTION OF WAVE FRONT TIME

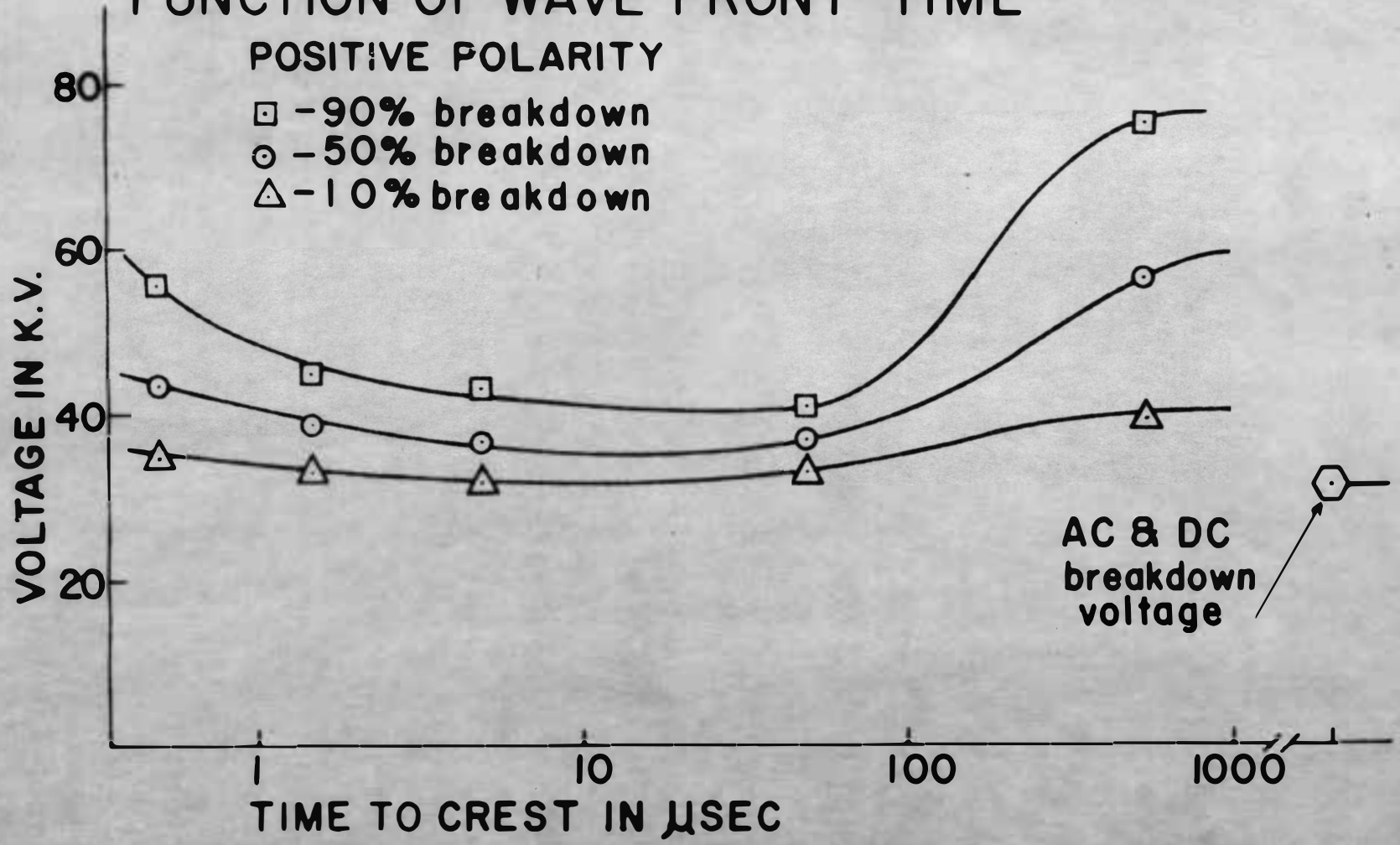


Fig. 21

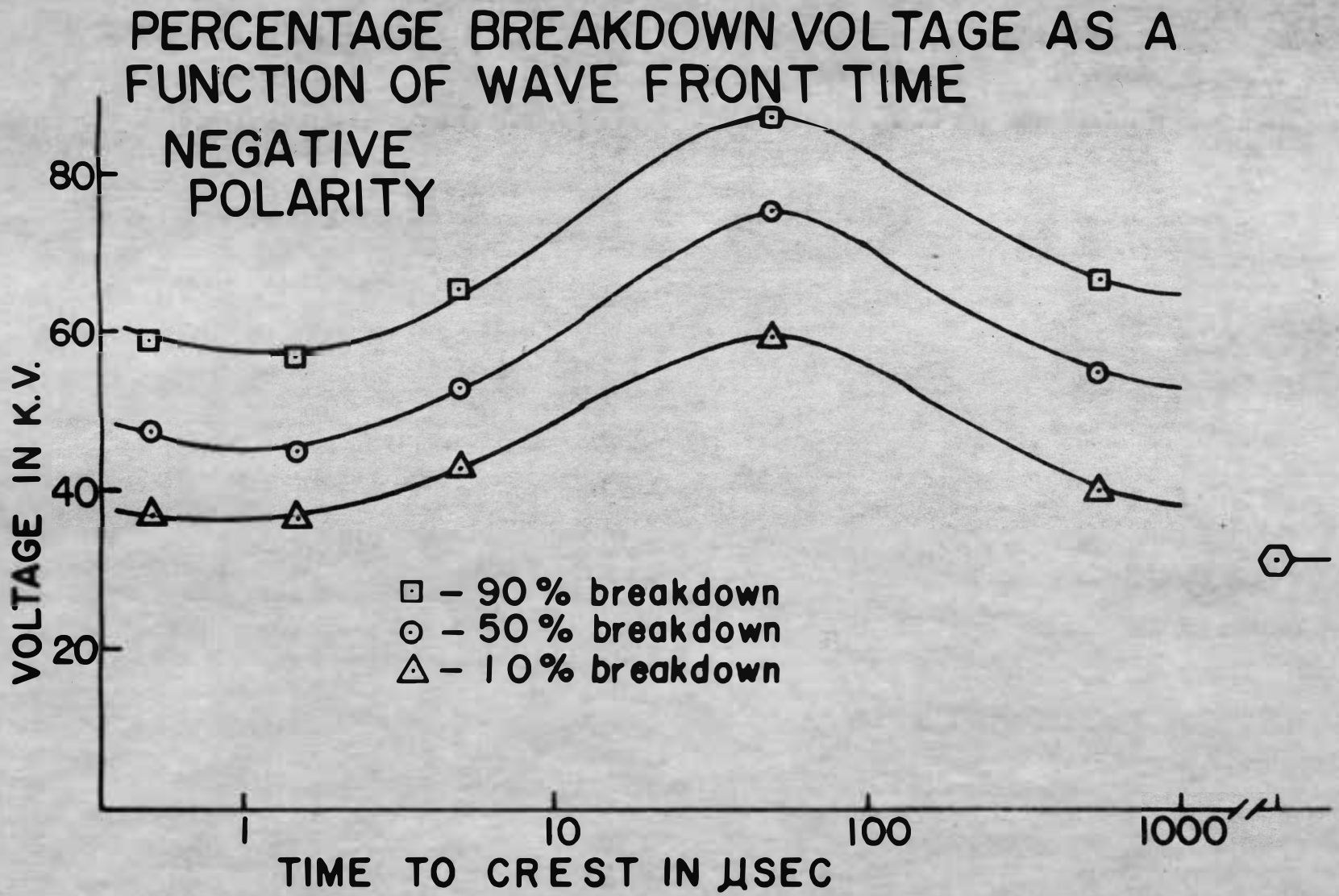
PERCENTAGE BREAKDOWN VOLTAGE AS A FUNCTION OF WAVE FRONT TIME
NEGATIVE POLARITY
80
60
40
20
VOLTAGE IN K.V.
□ – 90 % breakdown
⊙ – 50 % breakdown
△ – 10 % breakdown
1
10
100
1000
TIME TO CREST IN μSEC

Fig. 22

## Explanations of Results

The probability distribution form of the percentage breakdown versus applied voltage curves agrees with the concept of statistical time lags in the gap. If the appearance of an initiatory electron with high probability of causing breakdown is a statistical function of time, then in a given time, there will be a certain probability of its appearance. This critical time of appearance will be that time from when the voltage wave reaches a value such that breakdown can occur until the wave again recedes below this value. With voltage waves such as were applied in the present experiment, the critical time will increase as the crest value of the wave is increased. Thus, when breakdown percentage is plotted as a function of applied voltage, the form of the curve obtained could be expected to be a probability distribution curve.

The level of voltage that must be reached before the initiatory electron could cause breakdown is the D.C. breakdown voltage. This voltage is in accordance with both Townsend's Theory and Loeb and Meek's Theory.

If the supposition is made that the breakdown probability depends mostly on the D.C. voltage level and the time that the applied voltage stays above this level, then the following can be concluded. When different wave forms

are used, the percentage breakdown will depend on the time above the D.C. value and not the crest voltage. In other words, two waves having the same time above D.C. breakdown but different crest values, would have the same percentage of breakdowns.

The present investigation was carried out in part to test this supposition. There was a dependence of breakdown value on wave front time found but it is quite different than that supposed. At the shorter rise time waves, the percentage breakdown levels do decrease as rise time increases. As the rise times become longer, the levels rise again before falling off to lower values at much longer times.

An explanation of this phenomenon was proposed as follows. For the faster rise time waves, it was suggested that the breakdown voltage level was reached before the photo-electrons in the gap region were swept out by the applied voltage. However, with the longer wavefronts, more time was available to clear the region of photo-electrons. The probability of an initiatory electron appearing in the gap would be a function of the photo-electron density in the gap region. This density would be reduced more for a slower wave rise time than a faster one. When the wave front time is very long, the density will be low in the region, but the wave is rising slowly and will not reach

such a high value before the right electron is produced by gamma radiation. Support for this idea is shown by the scattering of data for long waves.

It can be assumed that most of the photo-electrons in the region are produced by interactions of the gamma rays passing through the region. The count rate of these rays was 3,200 per second or about one every 100 microseconds. If it is assumed that every count produces an electron, which is not quite true, then it can be seen that it will be quite awhile between electrons as far as a 5 x 10 microsecond wave is concerned. But the lifetime of these electrons is quite long. In most cases, the electron will diffuse out of the region of interest before it is recaptured into a molecule. It would seem that the diffusion process is a very important part of the whole problem. Under static conditions, the gap region will contain a certain density of photo-electrons, and the density will be kept uniform by diffusion. When any voltage wave is applied to the gap, the small volume directly centered in the gap will be swept free of electrons almost immediately. The electrons in the region of the gaps will begin diffusing into the gap volume and begin being swept out by the field. So the length of time the wave is applied, before it reaches a level sufficient for probably breakdown, will determine what the

photo-electron density and density gradient, at the time that voltage level is reached, will be in the gap region.

Experimental evidence supporting the above ideas was accidentally found by this author. While running a cycle of the 0.5 x 10 microsecond voltage wave tests, the high voltage D.C. source was energized in the test area. The output terminal of this test set was suspended about one and one-half feet above the test cell. The D.C. voltage was raised to a value such that corona was clearly visible at the terminal. The level of the 0.5 x 10 wave being applied at that time was sufficient for breakdown on every trial. After the D.C. set had been energized for a minute or so and shut off, the gap could not be broken down by the impulse wave at all, at that voltage level. The wave was applied at the same level every 30 seconds for the next 10 minutes before any breakdowns occurred. Once breakdown did occur, the level was sufficient for 100% breakdown again. The D.C. field established over the region of the test cell must have removed all photo-electrons in the region. A long time then had to elapse before the electron density came back to normal again and breakdown could again occur.

The above proposed explanation of the hump in the volt-time curves for nitrogen shown in Figures 21 and 22, is probably subject to criticism. A detailed analysis into the

problem would require that consideration be given to electrons produced by gamma rays striking the glass walls of the test cell and the electrodes, and electrons being produced by thermal emission from the electrodes. What the probability of producing electrons by gamma rays in any of the above substances would be, would also have to be considered. The diffusion rates would have to be known for the electron not only in the gas but also through the walls of the glass test cell.

Considerations of these factors and probably some others missed or omitted by this author would be needed in order to completely specify a solution to the problems. A complete analysis would have to be able to account for many things not yet mentioned such as why there are different curves for different applied voltage polarities. Also, it was noted that the curves of per cent breakdown versus applied voltage have the form of probability distribution curves. It should also be noted that since they are not true probability distribution curves, the relationship is not entirely statistical in nature. This means other non-statistical factors are present which are not accounted for here.

This author has not had time or equipment to consider a detailed investigation of all these factors at this time.

## Correlation of Results with Other Investigators

An investigation of the relationship of applied voltage time to breakdown strength of solid insulation was carried out by V. M. Montsinger in 1935. His results are shown by the curve in Figure 23. The curves obtained in this experiment would correspond to the first portion of Figure 23. More work needs be done here before a complete comparison can be made. The difference in relative time strengths can be easily noted. The solid insulation strength declines with time except for the flat strength portion. It has no humps in it as the nitrogen curve does.[26]

The hump in the volt-time curve for gases has been established by many investigators.[27] Huges and Roberts found that the per cent breakdown voltage varies with wave-front time. The curve they show has very much the same shape as the one found in the present paper. They used a different electrode configuration (rod-rod and rod-plane gaps) and different wave times than used here. The similarity of results would indicate the phenomenon is a gas characteristic and not dependent on electrodes. They gave no theoretical explanations for the shape of their curves.[28]

Walters and Jones also found that wave-front time had an effect on percentage breakdown levels. Their investigation was concerned with very long gaps (30 inches), so

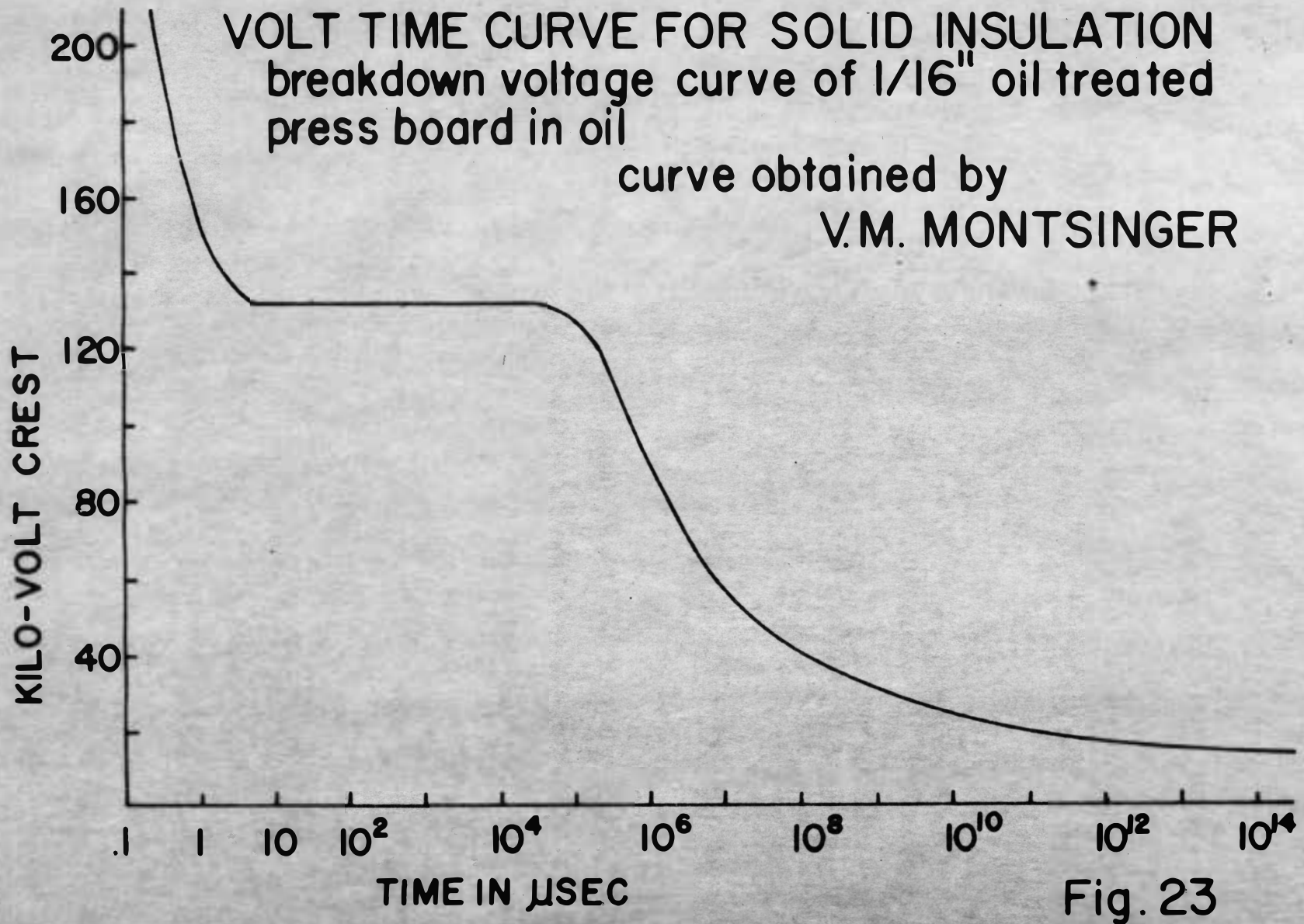
VOLT TIME CURVE FOR SOLID INSULATION
breakdown voltage curve of 1/16" oil treated press board in oil
curve obtained by
V.M. MONTSINGER
KILO-VOLT CREST
200
160
120
80
40
.1
1
10
$10^2$
$10^4$
$10^6$
$10^8$
$10^{10}$
$10^{12}$
$10^{14}$
TIME IN μSEC

Fig. 23

the results were not comparable to this paper. Their volt-time curve did not vary in a smooth manner and so no general shape could be determined.[29]

An investigation of the effect of approach voltage on statistical time lags in air and $SF_6$ and mixtures of these was carried out by Binns and Daryan. They superimposed an impulse wave on top of a D.C. voltage. They state that little effect on time lag was found due to changing D.C. approach voltage levels. Their data shows that as approach voltage is varied from 0 to 80% of D.C. breakdown, the average time lag goes from 45 to 75 microseconds for air and from 65 to 90 microseconds for $SF_6$. This is an increase of about 70% for air and 50% for $SF_6$. This author contends that approach voltage does have an effect on time lag. This increase would correspond to the differences in breakdown for short and long front voltage waves as discussed previously.[30]

# CONCLUSIONS

The curves of percentage breakdown voltage versus wave-front risetime shown in Figures 21 and 22 represent the breakdown characteristic of nitrogen under varying wave fronts. These curves can be used to compare the relative strength of nitrogen (or its equivalent air) with any gases (including electro-negative gases) under the same test conditions. More points should be taken on the nitrogen curves at long wave fronts to more definitely define the shape of the curve and find where the positive polarity begins to descend.

The shape of the percentage breakdown voltage versus wave risetime curve is much different for the gas tested (nitrogen) than that generally recognized for solid insulations, especially in the midrange, switching surge region. The ratio of the midrange, switching surge, breakdown voltage to the D.C. breakdown voltage, is about 230% while it is of the order of 850% of the D.C. breakdown voltage for solids.

In this report, as in the literature, the percentage breakdown voltage was plotted as a function of voltage wave risetime. It is believed by this author that if the time to one-half crest on the waveback is 10 to 20 times the risetime or more, the length will have little effect

on the breakdown value. This effect should be investigated and determined more precisely.

The theoretical reasons for the shape of the volt-time curve is open to more investigation and discussion. Proposed in this paper are some explanations (see pages 59-63) of the shape of the curve in terms of the availability of initiatory electrons in the gap region. Much more work is needed to determine if these proposals are creditable or not.

## LITERATURE CITED


1. K. B. McEachron and K. B. Patrick, Playing with Lightning, New York: Random House Inc., (1940) pp. 3-26, 48-59.

2. American Standard for Measurement of Voltage in Dielectric Tests, AIEE Standard 4, A.S.A., C68.1, (1953).

   Proposed Guide for Transformer Impulse Test, AIEE Standard 93, (December, 1962)

3. Vei-Shi Chen Ho, "The Effect of Additives on Gaseous Insulation Under Electrical Stress", South Dakota State College, Brookings, South Dakota, Thesis, (June, 1961)

4. L. C. Whitman, "Impulse Voltage Tests on Air and $C_3F_8$," IEEE Transactions on Electrical Insulation, Volume EI-1 No. 2, (November, 1965).

5. L. C. Whitman and J. Tanaka, "Effect of Addition of $NF_3$ to $C_3F_8$," South Dakota State College, Brookings, South Dakota, (1963) Unpublished Article.

6. V. M. Montsinger, "Breakdown Curve for Solid Insulation" Electrical Engineering, Vol. 54, No. 12 (December, 1935) pp. 1300.

7. J. S. Townsend, Nature. 62, 340, (1900)
   J. S. Townsend, Phil. Mag. 1, 198, (1901)
   J. S. Townsend, Phil. Mag. 3, 557, (1902)
   J. S. Townsend, Electricity in Gases
   London, G.B. Oxford University Press, (1915)

8. J. Frank, Z. Physik, 25, 312, (1924)
   J. Frank and V. Behr, Verhandl.deut.physik.Ges., 16, 57, (1914)

9. L. B. Loeb, Fundamental Processes of Electrical Discharges in Gases, New York: John Wiley and Sons, (1939) pp. 372-410

10. P. O. Pedersen, Ann.de Physik, 71, 371 (1923)

11. K. K. Darrow, Electrical Phenomina in Gases, Baltimore: Williams and Wilkens Co. (1932) pp. 314-315

12. L. B. Loeb and J. M. Meek, The Mechanism of the Electric Spark, Stanford: University Press, (1941) pp. 34-107

13. F. Llewellyn-Jones, Ionization and Breakdown in Gases, New York: John Wiley and Sons, (1957) pp. 80-82

14. J. M. Meek and J. D. Craggs, Electrical Breakdown of Gases, London G.B.: Oxford University Press, (1953) pp. 282-288

15. I. S. Marshak, "Electrical Breakdown in Gases Close to Atmospheric Pressures," Soviet Physics Uspekui, Vol. 3, No. 4 (Jan.-Feb. 1961) pp. 625-651

16. H. Raether, Electron Avalanches and Breakdown in Gases, Washington D.C.: Butterworth Inc. (1964) pp. 114-143

17. L. B. Loeb, Electrical Coronas, Berkeley and Los Angeles: University of California Press, (1965) pp. 611-630

18. F. W. Peek, Jr., Dielectric Phenomina in High Voltage Engineering, New York: McGraw-Hill Book Co. Inc. (1929) pp. 142-145

19. K. Zuber, Ann.Physik 76, 231 (1925)
M. vonLaue, Ann.Physik 76, 261 (1925)

20. J. H. Hagenguth, "Volt-Time Areas of Impulse Spark-Over", AIEE Transactions, Vol. 60 (1941) pp. 803-810

21. J. D. Cobine, Gaseous Conductors, New York: Dover Publications Inc. (1958) pp. 186-193

22. W. O. Schumann, Elektrische Durchbruehfeldstarke vonGasen, Berlin: Springer-Verlag, (1923)

23. A. Pedersen, "Calculation of spark breakdown or corona starting voltages in non-uniform fields", Paper No. 31TP66-80, read at IEEE Winter Power Meeting, (Jan.1966)

24. J. M. Meek, "A Theoretical Determination of Breakdown Voltages for Sphere Gaps," Journal of Franklin Institute, Vol. 230 (1940)

25. M. L. Manning, "Gaseous Insulation: Its Importance and Need for Test Methods", ASTM Special Technical Publication No. 346, Alpha N.J., (1963) pp. 3-20

26. C. N. Works and D. Berg, "Portable 125 K.V. Impulse Generator", Insulation, Vol. 8, No. 12, (Nov. 1962), pp. 41-45

27. F. Turner, Engineer at General Electric high voltage lab, Pittsfield, Massachusetts, private communication (Jan. 28, 1966)

28. R. C. Hughes and W. J. Roberts, "Application of Flashover Characteristics of Air Gaps to Insulation Co-ordination", Proc. IEE, Vol. 112, No. 1 (Jan. 1965) pp. 198-202

29. R. T. Walters and R. E. Jones, "The Impulse Breakdown Voltage and Time-Lag Characteristics of Long Gaps in Air, I and II", Phil. Trans. A (G.B.), Vol. 256, No. 1069, (1964) pp. 185-234.

30. D. F. Binns and C. L. Dargan, "Statistical Time Lags in Mixtures of $SF_6$ and Air", Brit. J. Appl. Phys., Vol. 16, No. 2 (Feb. 1965) pp. 181-183

31. G. Francis, Ionization Phenomina in Gases, London: Butterworths Inc. (1960)

32. J. B. Hastad, Physics of Atomic Collisions, Washington D.C.: Butterworths Inc. (1964)

33. L. B. Loeb, Basic Processes of Gaseous Electronics, Berkeley and Los Angeles: University of California Press, (Second Edition, 1961)

# APPENDIX ONE

TABLE I. BACKGROUND GAMMA RADIATION COUNTS AS FUNCTION OF ENERGY 60 MINUTE COUNT TIME.

| Channel | Counts | Channel | Counts | Channel | Counts |
|---|---|---|---|---|---|
| 1 | 7467 | 36 | 1454 | 71 | 403 |
| 2 | 6304 | 37 | 1383 | 72 | 411 |
| 3 | 8301 | 38 | 1274 | 73 | 378 |
| 4 | 12550 | 39 | 1250 | 74 | 424 |
| 5 | 17559 | 40 | 1224 | 75 | 391 |
| 6 | 19077 | 41 | 1218 | 76 | 350 |
| 7 | 18593 | 42 | 1127 | 77 | 370 |
| 8 | 18148 | 43 | 1103 | 78 | 377 |
| 9 | 17258 | 44 | 1110 | 79 | 334 |
| 10 | 15758 | 45 | 951 | 80 | 342 |
| 11 | 14509 | 46 | 896 | 81 | 352 |
| 12 | 12756 | 47 | 934 | 82 | 357 |
| 13 | 11651 | 48 | 868 | 83 | 337 |
| 14 | 10441 | 49 | 940 | 84 | 323 |
| 15 | 9411 | 50 | 890 | 85 | 347 |
| 16 | 8481 | 51 | 856 | 86 | 314 |
| 17 | 7683 | 52 | 841 | 87 | 283 |
| 18 | 7128 | 53 | 763 | 88 | 306 |
| 19 | 6379 | 54 | 724 | 89 | 308 |
| 20 | 5615 | 55 | 660 | 90 | 309 |
| 21 | 5042 | 56 | 598 | 91 | 285 |
| 22 | 4579 | 57 | 578 | 92 | 254 |
| 23 | 4102 | 58 | 628 | 93 | 234 |
| 24 | 3775 | 59 | 549 | 94 | 257 |
| 25 | 3357 | 60 | 515 | 95 | 274 |
| 26 | 3125 | 61 | 485 | 96 | 263 |
| 27 | 3015 | 62 | 495 | 97 | 267 |
| 28 | 2756 | 63 | 494 | 98 | 253 |
| 29 | 2554 | 64 | 462 | 99 | 293 |
| 30 | 2245 | 65 | 448 | | |
| 31 | 2012 | 66 | 442 | Σ = 314357 | |
| 32 | 1783 | 67 | 438 | | |
| 33 | 1730 | 68 | 410 | per sec. = 87.32 | |
| 34 | 1561 | 69 | 414 | | |
| 35 | 1566 | 70 | 412 | | |

Each channel is $10.71 \times 10^3$ electron volts wide and channel one starts at $25 \times 10^3$ electron volts, 99 ends at $1085.7 \times 10^3$ electron volts.

TABLE II. GAMMA RAY COUNTS AT ELECTRODE POSITION WITH RADIUM SOURCE 18" DISTANT IN LEAD CAN AS A FUNCTION OF ENERGY COUNT TIME 20 MINUTES.

| Channel | Counts | Channel | Counts | Channel | Counts |
|---|---|---|---|---|---|
| 1 | 64038 | 36 | 39921 | 71 | 23677 |
| 2 | 59528 | 37 | 39079 | 72 | 22530 |
| 3 | 56117 | 38 | 38889 | 73 | 22266 |
| 4 | 58972 | 39 | 39031 | 74 | 21687 |
| 5 | 72065 | 40 | 39418 | 75 | 21000 |
| 6 | 80591 | 41 | 40454 | 76 | 20694 |
| 7 | 72468 | 42 | 41425 | 77 | 20228 |
| 8 | 70101 | 43 | 41879 | 78 | 19764 |
| 9 | 73119 | 44 | 40576 | 79 | 19717 |
| 10 | 75430 | 45 | 38719 | 80 | 19301 |
| 11 | 76890 | 46 | 37200 | 81 | 19082 |
| 12 | 78296 | 47 | 36469 | 82 | 19069 |
| 13 | 80507 | 48 | 36442 | 83 | 18586 |
| 14 | 82535 | 49 | 37903 | 84 | 18643 |
| 15 | 83852 | 50 | 39751 | 85 | 17727 |
| 16 | 85368 | 51 | 41243 | 86 | 17813 |
| 17 | 85359 | 52 | 41301 | 87 | 16621 |
| 18 | 82386 | 53 | 39549 | 88 | 16433 |
| 19 | 79028 | 54 | 36442 | 89 | 16233 |
| 20 | 72728 | 55 | 33222 | 90 | 15771 |
| 21 | 68437 | 56 | 30255 | 91 | 15710 |
| 22 | 63287 | 57 | 28486 | 92 | 15370 |
| 23 | 59895 | 58 | 27328 | 93 | 15783 |
| 24 | 57245 | 59 | 26406 | 94 | 15643 |
| 25 | 53912 | 60 | 25902 | 95 | 16004 |
| 26 | 52042 | 61 | 25850 | 96 | 16737 |
| 27 | 50341 | 62 | 25364 | 97 | 17815 |
| 28 | 47649 | 63 | 25552 | 98 | 18610 |
| 29 | 46590 | 64 | 25891 | 99 | 19234 |
| 30 | 45125 | 65 | 25647 | | |
| 31 | 43953 | 66 | 25978 | $\Sigma$ = 3,954,051 | |
| 32 | 43379 | 67 | 25753 | | |
| 33 | 42472 | 68 | 25358 | per sec = | |
| 34 | 40730 | 69 | 24462 | 3295.04 | |
| 35 | 40285 | 70 | 24423 | | |

TABLE III. GAMMA RAY COUNT AT ELECTRODE POSITION WITH RADIUM SOURCE IN TEST POSITION AND 2 GLASS CYLINDERS BETWEEN RADIUM AND ELECTRODE POSITION AS A FUNCTION OF ENERGY.

| Channel | Counts | Channel | Counts | Channel | Counts |
|---|---|---|---|---|---|
| 1 | 67500 | 36 | 37627 | 71 | 21288 |
| 2 | 56851 | 37 | 37045 | 72 | 20897 |
| 3 | 53955 | 38 | 36411 | 73 | 20648 |
| 4 | 57095 | 39 | 36044 | 74 | 19754 |
| 5 | 68010 | 40 | 36323 | 75 | 19190 |
| 6 | 76286 | 41 | 36708 | 76 | 18894 |
| 7 | 71416 | 42 | 37435 | 77 | 18485 |
| 8 | 72062 | 43 | 37568 | 78 | 18084 |
| 9 | 75907 | 44 | 37858 | 79 | 17679 |
| 10 | 78816 | 45 | 35928 | 80 | 17546 |
| 11 | 78912 | 46 | 34714 | 81 | 17456 |
| 12 | 78833 | 47 | 34037 | 82 | 17254 |
| 13 | 79651 | 48 | 33053 | 83 | 16831 |
| 14 | 80150 | 49 | 33257 | 84 | 16955 |
| 15 | 81171 | 50 | 33945 | 85 | 16517 |
| 16 | 82176 | 51 | 35886 | 86 | 16255 |
| 17 | 81085 | 52 | 36537 | 87 | 15476 |
| 18 | 77985 | 53 | 36121 | 88 | 15321 |
| 19 | 74919 | 54 | 34361 | 89 | 14613 |
| 20 | 68821 | 55 | 31598 | 90 | 14504 |
| 21 | 65341 | 56 | 28898 | 91 | 13911 |
| 22 | 60881 | 57 | 26545 | 92 | 14153 |
| 23 | 57263 | 58 | 25162 | 93 | 13976 |
| 24 | 54214 | 59 | 24496 | 94 | 13836 |
| 25 | 51983 | 60 | 23608 | 95 | 13883 |
| 26 | 50003 | 61 | 23605 | 96 | 14381 |
| 27 | 47891 | 62 | 23308 | 97 | 14723 |
| 28 | 46217 | 63 | 23021 | 98 | 15205 |
| 29 | 44754 | 64 | 23216 | 99 | 15751 |
| 30 | 43193 | 65 | 22904 | | |
| 31 | 42260 | 66 | 23353 | Σ = 3,738,891 | |
| 32 | 41037 | 67 | 23063 | | |
| 33 | 40323 | 68 | 22858 | per sec. = | |
| 34 | 39413 | 69 | 22095 | | |
| 35 | 38373 | 70 | 22090 | 3,115.7 | |

TABLE IV. VALUES OF PERCENTAGE BREAKDOWN AT THE APPLIED VOLTAGES INDICATED FOR THE 0.5 x 10 MICRO-SECONDS VOLTAGE WAVE.

Positive Polarity

| | | | | | | | |
|---|---|---|---|---|---|---|---|
| K.V. | 33.1 | 36.2 | 39.4 | 42.8 | 45.8 | 48.9 | 52.3 |
| % | 0.0 | 10.0 | 33.3 | 43.3 | 67.3 | 78.3 | 80.0 |

| | | | |
|---|---|---|---|
| K.V. | 55.3 | 58.5 | 61.9 |
| % | 83.3 | 90.0 | 100.0 |

Negative Polarity

| | | | | | | | |
|---|---|---|---|---|---|---|---|
| K.V. | 34.9 | 37.5 | 40.2 | 42.8 | 45.4 | 48.2 | 50.8 |
| % | 1.6 | 6.6 | 31.6 | 25.0 | 45.0 | 65.0 | 65.0 |

| | | | | |
|---|---|---|---|---|
| K.V. | 53.3 | 56.1 | 58.5 | 61.3 |
| % | 65.0 | 81.6 | 86.6 | 100.0 |

TABLE V. VALUES OF PERCENTAGE BREAKDOWN AT THE APPLIED VOLTAGES INDICATED FOR THE 1.5 x 40 MICRO-SECONDS VOLTAGE WAVE.

Positive Polarity

| | | | | | | | |
|---|---|---|---|---|---|---|---|
| K.V. | 32.3 | 33.5 | 34.6 | 35.8 | 37.0 | 38.1 | 39.2 |
| % | 3.3 | 11.6 | 10.0 | 30.0 | 48.3 | 50.6 | 58.3 |

| | | | | | | |
|---|---|---|---|---|---|---|
| K.V. | 40.3 | 41.5 | 42.7 | 43.8 | 45.0 | 46.2 |
| % | 65.0 | 70.0 | 81.6 | 83.3 | 88.3 | 95.0 |

Negative Polarity

| | | | | | | | |
|---|---|---|---|---|---|---|---|
| K.V. | 35.0 | 37.2 | 39.4 | 41.5 | 43.7 | 45.8 | 47.8 |
| % | 0 | 11.6 | 20.0 | 38.3 | 41.6 | 51.6 | 66.6 |

| | | | | | |
|---|---|---|---|---|---|
| K.V. | 50.0 | 52.2 | 54.3 | 56.5 | 58.7 |
| % | 63.6 | 71.6 | 83.3 | 90.0 | 96.6 |

TABLE VI. VALUES OF PERCENTAGE BREAKDOWN AT THE APPLIED VOLTAGES INDICATED FOR THE 5 x 100 MICRO-SECONDS VOLTAGE WAVE.

Positive Polarity

| | | | | | | | |
|---|---|---|---|---|---|---|---|
| K.V. | 31.8 | 32.8 | 34.0 | 35.2 | 36.4 | 37.5 | 38.7 |
| % | 8.3 | 13.3. | 26.6 | 36.6 | 50.0 | 61.6 | 66.6 |

| | | | | | |
|---|---|---|---|---|---|
| K.V. | 39.9 | 41.0 | 42.2 | 43.4 | 44.6 |
| % | 81.6 | 75.0 | 90.0 | 86.6 | 98.3 |

Negative Polarity

| | | | | | | | |
|---|---|---|---|---|---|---|---|
| K.V. | 40.0 | 41.9 | 43.9 | 46.1 | 48.1 | 50.2 | 52.2 |
| % | 3.3 | 8.3 | 20.0 | 13.3 | 40.0 | 38.3 | 48.3 |

| | | | | | | |
|---|---|---|---|---|---|---|
| K.V. | 54.2 | 56.3 | 58.3 | 60.4 | 62.4 | 64.4 |
| % | 66.6 | 55.0 | 65.0 | 78.3 | 81.6 | 93.3 |

TABLE VII. VALUES OF PERCENTAGE BREAKDOWN AT THE APPLIED VOLTAGE LEVELS INDICATED FOR THE 50 x 1000 MICROSECONDS VOLTAGE WAVE.

Positive Polarity

| | | | | | | | |
|---|---|---|---|---|---|---|---|
| K.V. | 32.9 | 34.1 | 35.2 | 36.2 | 37.3 | 38.3 | 39.3 |
| % | 6.6 | 18.3 | 26.6 | 45.0 | 56.6 | 66.6 | 81.6 |

| | | |
|---|---|---|
| K.V. | 40.4 | 41.6 |
| % | 90.0 | 93.3 |

Negative Polarity

| | | | | | | | |
|---|---|---|---|---|---|---|---|
| K.V. | 55.6 | 57.6 | 59.6 | 61.6 | 63.8 | 65.8 | 67.8 |
| % | 3.3 | 13.3 | 10.0 | 11.6 | 20.0 | 21.6 | 26.6 |
| K.V. | 70.1 | 72.0 | 74.3 | 76.3 | 78.2 | 80.2 | 81.8 |
| % | 31.6 | 46.6 | 43.3 | 75.0 | 65.0 | 58.3 | 70.0 |

| | | | | |
|---|---|---|---|---|
| K.V. | 83.5 | 85.1 | 86.8 | 88.1 |
| % | 73.3 | 83.3 | 86.6 | 93.3 |

TABLE VIII. VALUES OF PERCENTAGE BREAKDOWN AT THE APPLIED VOLTAGE INDICATED FOR THE 550 x 9000 MICROSECONDS VOLTAGE WAVE.

**Positive Polarity**

| | | | | | | | |
|---|---|---|---|---|---|---|---|
| K.V. | 40.0 | 42.0 | 44.1 | 46.0 | 48.2 | 50.3 | 52.5 |
| % | 20.0 | 11.6 | 24.3 | 24.3 | 30.0 | 36.6 | 41.6 |
| K.V. | 54.7 | 56.6 | 58.8 | 60.7 | 62.9 | 65.0 | 67.0 |
| % | 56.6 | 50.0 | 50.0 | 61.6 | 65.0 | 75.0 | 73.3 |

| | | |
|---|---|---|
| K.V. | 69.1 | 71.1 |
| % | 80.0 | 83.3 |

**Negative Polarity**

| | | | | | | | |
|---|---|---|---|---|---|---|---|
| K.V. | 33.7 | 35.9 | 38.1 | 40.0 | 42.0 | 44.1 | 46.0 |
| % | 0.0 | 0.0 | 18.8 | 7.7 | 12.3 | 22.1 | 27.2 |
| K.V. | 48.2 | 50.3 | 52.5 | 54.7 | 56.6 | 58.8 | 60.7 |
| % | 33.6 | 36.7 | 50.6 | 60.6 | 72.2 | 69.3 | 82.6 |
| % | | | | | | | 87.5 |
| K.V. | 62.9 | 65.0 | 67.0 | 69.1 | 70.8 | 72.5 | 74.2 |
| % | 62.5 | 57.5 | 50.0 | 50.0 | 70.0 | 95.0 | 100.0 |
| % | 86.4 | 89.0 | 91.9 | 91.0 | 94.5 | 99.1 | 100.0 |

TABLE IX. VALUES OF DIFFERENT PERCENTAGE BREAKDOWN POINTS IN K.V. VERSUS THE TIME TO CREST OF THE DIFFERENT WAVES.

Positive Polarity

| $t_1$ | 10% point | 50% point | 90% point |
|---|---|---|---|
| 0.5 | 34.7 | 43.8 | 55.7 |
| 1.5 | 33.4 | 38.3 | 45.3 |
| 5.0 | 31.9 | 36.5 | 42.9 |
| 50.0 | 33.3 | 36.8 | 40.7 |
| 550.0 | 39.8 | 56.1 | 75.7 |
| A.C. | | 31.6 crest | |
| D.C. | | 31.8 | |

Negative Polarity

| $t_1$ | 10% point | 50% point | 90% point |
|---|---|---|---|
| 0.5 | 37.1 | 47.6 | 59.0 |
| 1.5 | 36.7 | 45.3 | 56.6 |
| 5.0 | 42.5 | 52.7 | 65.5 |
| 50.0 | 59.6 | 75.5 | 87.5 |
| 550.0 | 40.0 | 54.7 | 66.9 |
| A.C. | | 31.6 crest | |
| D.C. | | 31.8 | |

# APPENDIX TWO

## THEORETICAL ANALYSIS OF WAVE SHAPING CIRCUIT

An equivalent circuit of the impulse generator charged and ready to be triggered is shown in Figure 24. The switch is closed by the arcs in the generator.

Summing the voltage drops in the direction of current around the loops using Laplace transformed variables; the following is obtained:

In Loop 1.

$$-\frac{E_o}{s} + \frac{I_1}{sC_1} + I_1R_1 + \frac{I_1}{sC_2} - \frac{I_2}{sC_2} = 0 \qquad (1)$$

In Loop 2.

$$-\frac{I_1}{sC_2} + \frac{I_2}{sC_2} + I_2R_2 = 0 \qquad (2)$$

from (1)

$$I_1 = \left(\frac{E_o}{s} + \frac{I_2}{sC_2}\right) \Big/ \left(\frac{1}{sC_1} + \frac{1}{sC_2} + R_1\right) \qquad (3)$$

from (2)

$$I_2 = \frac{I_1}{sC_2} - \left(R_2 + \frac{1}{sC_2}\right) = \frac{I_1}{(R_2C_2s + 1)} \qquad (4)$$

Substitute (3) in (4)

$$I_2 = \frac{1}{(R_2C_2s + 1)} \cdot \frac{\left(\frac{E_o}{s} + \frac{I_2}{sC_2}\right)}{\left(R_1 + \frac{1}{sC_1} + \frac{1}{sC_2}\right)}$$

$$I_2 = \frac{E_oC_1}{R_1R_2C_1C_2s^2 + (R_2C_2 + R_2C_1 + R_1C_2)s + 1} \qquad (5)$$

# IMPULSE GENERATOR EQUIVALENT CIRCUIT

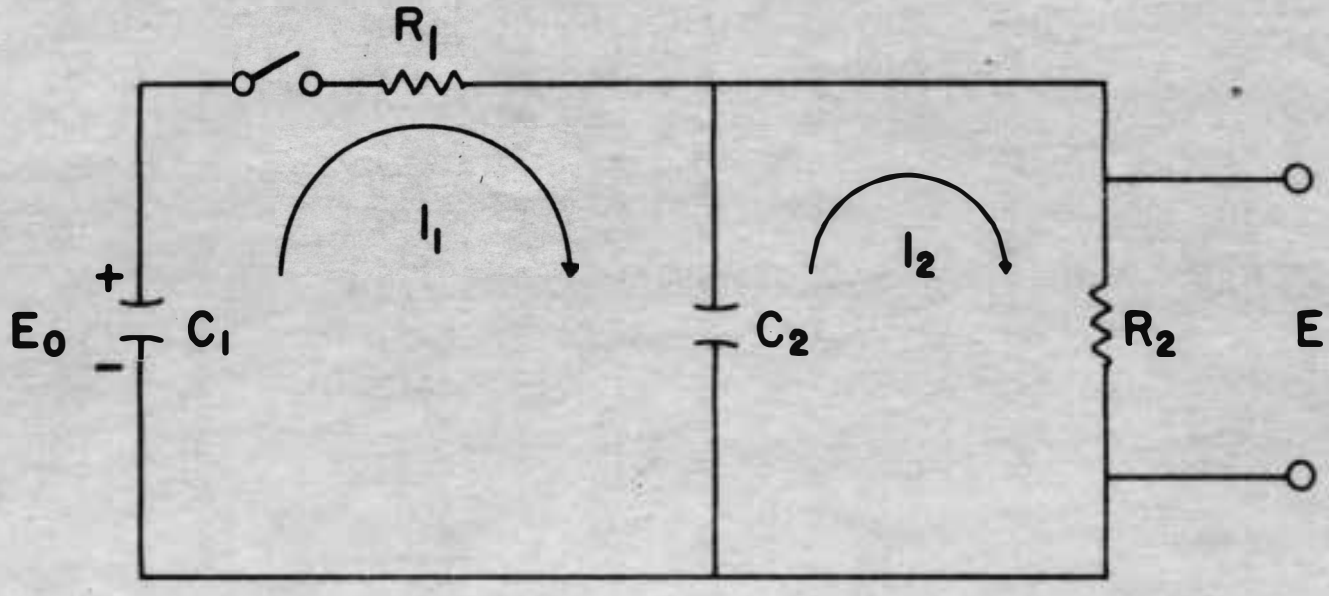


Fig. 24

Now

$$E = I_2 R_2 \tag{6}$$

Substitute (5) in (6) and rearrange

$$E = \frac{E_o}{R_1 C_2} \; \frac{1}{s^2 + \left(\frac{1}{R_1 C_2} + \frac{R_1 + R_2}{R_1 R_2 C_1}\right) s + \frac{1}{R_1 R_2 C_1 C_2}} \tag{7}$$

let

$$K_1 = \left(\frac{1}{R_1 C_2} + \frac{R_1 + R_2}{R_1 R_2 C_1}\right) \quad \text{and} \quad K_2 = \frac{1}{R_1 R_2 C_1 C_2} \tag{8}$$

Substitute (8) in (7)

$$E = \frac{E_o}{R_1 C_2} \; \frac{1}{s^2 + K_1 s + K_2} \tag{9}$$

The inverse Laplace Transform of this is:

$$L^{-1}\left[\frac{1}{s^2+2as+b^2}\right] = \frac{1}{(b^2-a^2)^{1/2}} \; e^{-at} \sin(b^2-a^2)^{1/2} t$$

Applying this to equation (9)

$$e(t) = \frac{E_o}{R_1 C_2}\left[\left(K_2 - \frac{K_1^2}{4}\right)^{1/2}\right] e^{-\frac{K_1}{2}t} \times$$

$$\left[\sin\left(K_2 - \frac{K_1^2}{4}\right)^{1/2} t\right] \tag{10}$$

let

$$\frac{E_o}{R_1 C_2} = A_1, \quad \left(K_2 - \frac{K_1^2}{4}\right)^{1/2} = A_2 \tag{11}$$

Substitute (11) into (10)

$$e(t) = \frac{A_1}{A_2} \; e^{-\frac{K_1}{2} t} \; \sin A_2 t \tag{12}$$

To obtain the risetime of this wave, equation (12) is differentiated with respect to t, set equal to zero and solved for $t_1$:

$$\frac{de(t)}{dt} = \frac{A_1}{A_2} - \frac{K_1}{2} e^{-\frac{K_1}{2} t_1} \sin A_2 t_1 + e^{-\frac{K_1}{2} t_1} \cos A_2 t_1 A_2 \qquad (13)$$

Set equal to zero and rearrange.

$$\frac{K_1}{2} \sin A_2 t_1 = A_2 \cos A_2 t_1 \qquad (14)$$

Dividing by $\frac{K_1}{2} \cos A_2 t_1$

$$\text{Tan } A_2 t_1 = \frac{2A_2}{K_1}$$

or

$$t_1 = \frac{1}{A_2} \text{ arc tan } \frac{2A_2}{K_1} \qquad (15)$$

where $K_1$ and $A_2$ are defined above.

When appropriate values were substituted into (15), it was found that

$$\frac{K_1^2}{4} > K_2$$

This made $A_1$ an imaginary quantity. The following change was made to take care of this problem:

In (14), if $iA_2$ is substituted for $A_2$

$$\frac{K_1}{2} \sin iA_2 t_1 = iA_2 \cos iA_2 t \qquad (16)$$